TECHNICAL REPORT

DEPARTMENT OF PHYSICS

UNIVERSITY OF CALIFORNIA

LOS ANGELES

CONTRACT RESEARCH

SPONSORED BY

OFFICE OF NAVAL RESEARCH

STUDY OF ACOUSTIC STREAMING

by

Herman Medwin

Technical Report No. VIII
December 1953

Submitted by

R. W. Leonard, Project Director

Office of Naval Research
Contract N6 onr-27507
Project NR014 - 302

Department of Physics
University of California
Los Angeles, California

TABLE OF CONTENTS

I. THEORY OF SURFACE AND VOLUME SOURCES OF VORTICITY IN ACOUSTIC FIELDS

A. INTRODUCTION

When a sound beam passes through a viscous fluid, vorticity is generated as a second-order effect and streaming results. An expression for these direct current streams has been derived by Eckart.[1] His equation (25a) is based on the hypotheses that $b = 4/3 + \mu'/\mu$ and the dynamic shear viscosity, $\mu = \rho\nu$, are both constant for the fluid density variations which accompany passage of a sound wave, and that the curl of the first-order particle velocity is zero ($\nabla \times \vec{u}_1 = 0$). Here, ρ is the density, $\nu' = \mu'/\rho$ is the kinematic bulk viscosity, and ν is the kinematic shear viscosity.

The assumption of the density independence of μ and μ' bears investigation. It is certainly true that in general one does not expect μ or μ' to be constant in a sound field, but it is not clear what effect, if any, their variation will have on streaming. The effect of variable μ is left for a future study; but a discussion of density dependent μ' is included here, and it will be shown that the vorticity equation is independent of such variation.

The second assumption, namely, $\nabla \times \vec{u}_1 = 0$, is an important one. It is probably permissible in the case considered by Eckart because the departure from irrotational behavior is small if the beam is completely "immersed" in the medium. However, if the sound beam makes

contact with a solid surface (say, a solid obstacle within the sound field, or an enclosing tube), then the particle velocity falls rapidly to zero in a transverse direction within a thin boundary layer measured by the viscous wavelength. Here viscous forces become relatively important, a velocity potential no longer exists, and the assumption $\nabla \times \vec{u}_1 = 0$ is certainly not valid. Actually, this nonzero value of the curl becomes most significant in such cases and is, in fact, necessary for the occurrence of the streaming discussed by Rayleigh,[2] Schuster and Matz,[3] and Schlichting.[4] It will be shown that there are three sources of vorticity: $\vec{S}_E$, a term identical to the Eckart source of vorticity; $\vec{S}_R$, the Rayleigh term, which appears when the acoustic field is rotational (principally at solid surfaces where the relative quiescence of the medium is described by the "boundary layer"); and $\vec{S}_T$, a third term, new to discussions of streaming, which has a nonzero value only when the acoustic field is rotational.

Finally, a distinction is made between "surface sources" of vorticity ($\vec{S}_R$ and $\vec{S}_T$) and "volume sources" of vorticity ($\vec{S}_E$), and solutions are cited for common situations in which the surface sources dominate the streaming.

B. SOURCES OF VORTICITY

In the formulation of the Navier-Stokes equations given by Lamb[5] a typical component equation is

$$\rho \frac{Du}{Dt} = -\partial p/\partial x + \partial/\partial x \left[\lambda \nabla \cdot \vec{u} + 2\mu \frac{\partial u}{\partial x}\right] + \partial/\partial y \left[\mu\left(\frac{\partial v}{\partial x} + \frac{\partial u}{\partial y}\right)\right]$$

$$+ \partial/\partial z \left[\mu\left(\frac{\partial u}{\partial z} + \frac{\partial w}{\partial x}\right)\right] \qquad (1)$$

and one is confronted immediately with the decision of whether or not $\lambda = -\frac{2}{3}\mu + \mu'$ and μ are to be considered functions of position and time (and thereby functions of density). Here λ is the dilatational viscosity, μ is the dynamic shear viscosity in poises, and μ' is called the dynamic bulk viscosity. ρ is the fluid density, $\vec{u}$ is the vector velocity with components u, v, w in the rectangular coordinate frame x, y, z. D/Dt is the hydrodynamic operator $(d/dt + \vec{u}\cdot\nabla)$. P is the mean external pressure on the volume element. Both Eckart and Rayleigh have considered that μ and μ' are independent of density at this point. In the following derivation of a more general equation which predicts streaming, μ will be considered constant, but the effect of variation of μ' with density will be considered by the expansion

$$\mu' = \mu'_o + (d\mu'/d\rho)_o \rho_1 = \mu'_o + \mu'_1 \tag{1a}$$

where μ'_o is the bulk viscosity at equilibrium density; ρ_1 is the first-order, acoustic, density; $(d\mu'/d\rho)_o$ represents the evaluation at equilibrium density. Then the vector force equation is

$$\rho_o(\partial\vec{u}/\partial t) + \rho_o\vec{u}\cdot\nabla\vec{u} = -\nabla P + (4/3\mu+\mu')\ \nabla\nabla\cdot\vec{u} - \mu\nabla\times(\nabla\times\vec{u}) + (\nabla\mu')(\nabla\cdot\vec{u}) \tag{2}$$

The notation ρ_1 and $\vec{u}_1$ will be used for the acoustic density and particle velocity, respectively, and $\vec{u}_2$ for the second-order particle velocity, the time average of which gives the stream velocity. Then the first-order continuity equation,

$$\partial\rho_1/\partial t + \rho_o\nabla\cdot\vec{u}_1 = 0 \tag{2a}$$

and the first-order force equation,

$$\rho_o \partial\vec{u}_1/\partial t = - c_o^2 \nabla\rho_1 + (4/3\mu_o+\mu_o')\nabla\nabla\cdot\vec{u}_1 - \mu_o \nabla\times(\nabla\times\vec{u}_1) \tag{3}$$

are the same as in Eckart's development. However, the second-order force equation becomes (assuming the pressure is a function of density only):

$$\rho_o \partial\vec{u}_2/\partial t+\rho_1 \partial\vec{u}_1/\partial t+\rho_o(\vec{u}_1\cdot\nabla)\vec{u}_1 = -c_o^2\nabla\rho_2 - c_o(dc/d\rho)_o\nabla(\rho_1^2)+(d\mu'/d\rho)_o(\nabla\cdot\vec{u}_1)\nabla\rho_1$$
$$+(4/3\mu_o+\mu_o')\nabla\nabla\cdot\vec{u}_2+(4/3\mu_1+\mu_1')\nabla\nabla\cdot\vec{u}_1 \tag{4}$$
$$-\mu_o\nabla\times\nabla\times\vec{u}_2 - \mu_1\nabla\times\nabla\times\vec{\mu}_1$$

With the assumption μ = constant, $\mu_1 = (d\mu/d\rho)_o\rho_1 = 0$. Further simplification results by introduction of $\rho_1(d\vec{u}_1/dt)$ from Eq. (3), so that when the curl of Eq. (4) is taken, and only the steady state is considered, there results the general vorticity equation:

$$\nabla^2\vec{R}_2 = \underbrace{+\,(-1/\rho_o^2)\,(4/3+\mu_o'/\mu_o)\nabla\rho_1\times\nabla(\partial\rho_1/\partial t)}_{\vec{S}_E}$$
$$+\underbrace{(-\rho_o/\mu_o)\nabla\times(\vec{u}_1\times\vec{R}_1)}_{\vec{S}_R}+\underbrace{(-1/\rho_o)\nabla\times(\rho_1\nabla\times\vec{R}_1)}_{\vec{S}_T} \tag{5}$$

in which $\vec{R}_2 = \nabla\times\vec{u}_2$ and $\vec{R}_1 = \nabla\times\vec{u}_1$. (It is noted that even if the medium fails to satisfy Hooke's law so that $(dc/d\rho)_o$ has a nonzero value, this term is multiplied by $\nabla(\rho_1^2)$, so that when the vorticity Eq. (5) is formed the term vanishes. This fact supports Eckart's omission of this effect in his study of the influence of viscosity on vorticity.) Equation (5) is a general equation which predicts steady-state streaming on the basis of μ being considered constant but with no assumption as to the constancy of μ', and for any acoustic field, irrotational or not.

If an irrotational sound field is assumed, $\vec{S}_R = \vec{S}_T = 0$ and what

remains is Eckart's Eq. (25a), where he uses the definition $b = 4/3 + \mu'/\mu$. It is noteworthy that the possibility of variation of bulk viscosity with density, which is considered here, does not affect the sources of vorticity. It is clear from Eq. (5) that the case $\vec{R}_1 = 0$ is a natural one to consider when one is interested, as Eckart was, in determining the bulk viscosity μ'.

To discuss the approach of other workers in streaming, it is convenient to recast Eq. (5) in terms of the kinematic coefficients $\nu = \mu/\rho$ and $\nu' = \mu'/\rho$. Observing that, for constant μ, $d\nu/d\rho = -\mu/\rho^2$, Eq. (5) becomes

$$\nabla^2\vec{R}_2 = \underbrace{+ (1/\rho_o\nu_o)(d\nu/d\rho)_o\ (4/3 + \nu'/\nu)\nabla\rho_1 x \nabla\partial\rho_1/\partial t}_{\vec{S}_E}$$

$$\underbrace{+ (-1/\nu_o)\nabla x\ (\vec{u}_1 x \vec{R}_1)}_{\vec{S}_R} + \underbrace{(1/\nu_o)(d\nu/d\rho)_o \nabla\ x(\rho_1 \nabla x \vec{R}_1)}_{\vec{S}_T} \qquad (6)$$

Rayleigh,[2] and Schuster and Matz[3] started with Eq. (2) in which μ' as well as μ was implicitly considered as constant. But then, in taking the curl to form the vorticity equation, they considered a rotational acoustic field and took ν and ν' constant. (Actually, Schuster and Matz put $\nu' = 0$.) It is clear that only the term $\vec{S}_R$ would remain after these assumptions, and this is precisely the driving term which Schuster and Matz obtain when they re-solve the Rayleigh problem of streaming in a tube, using vector notation. The assumptions of μ = constant and $\nu = \mu/\rho$ = constant are equivalent to assumping ρ = constant for the viscous stress terms, only. In both works, the authors apply their results to a compressible fluid

in which $\rho_1 \neq 0$. Schuster and Matz report an experimental check within about 20 per cent of theoretical predictions for the axial stream velocity halfway between loop and node in a standing wave in an air-filled cylindrical tube.

In addition to these two cases of streaming in a tube,[2,3] a search of the literature reveals one other type of streaming problem, involving oscillatory motion of the fluid at a solid surface, which has been solved; namely, a rigid cylinder vibrating in static fluid.[4] Schlichting has made the assumptions ν = constant, $\nu' = 0$ and an incompressible fluid; consequent $\vec{S}_E$ and $\vec{S}_T$ would be zero, and the only term which could contribute is $\vec{S}_R$. (Note: Schlichting's development which leads to a streaming velocity does not parallel the usual approach described here and in other references. He obtains experimental qualitative agreement with his theoretical solution.)

It is noted that $\vec{S}_T$, the third term of Eq. (5), is new to discussions of streaming phenomena. It does not appear when one assumes that the acoustic field is irrotational or if one assumes that ρ is constant in the viscous stress terms during passage of a sound wave.

In no case in the past have the authors made a critical evaluation of the magnitudes of the different sources of vorticity, although it is clear that the assumption $\nabla \times \vec{u}_1 \neq 0$ is essential to all three solutions[2-4] in which the acoustic field was in contact with a solid boundary. Two additional specific cases have been considered by the author; the streaming caused by (A) a plane progressive wave in which $\lambda_{viscous} \ll$ tube radius $\lesssim \lambda_{acoustic}$ and (B) a small rigid fixed sphere in a plane progressive wave. The solution to

problem (A) is presented in the appendix. At this time, however, it is possible to point out a distinction which should be made between surface sources of vorticity and volume sources of vorticity. The descriptive title "surface sources" is used for all sources of vorticity which depend, for their existence, on $\nabla \times \vec{u}_1 \neq 0$ (i.e. $\vec{S}_R$ and $\vec{S}_T$), and the title "volume source" for the source of vorticity which exists even when the acoustic field is assumed to be irrotational in character (i.e. $\vec{S}_E$). The significance of the terminology is this: The terms $\vec{S}_R$ and $\vec{S}_T$, depending as they do on $\nabla \times \vec{u}_1$ become extremely strong in the neighborhood of solid surfaces where the viscous forces are relatively important, a potential-type field does not exist, and large values of $\nabla \times \vec{u}_1$ are generated. On the other hand, $\vec{S}_R$ and $\vec{S}_T$ are probably negligible in regions many viscous wavelengths distant from the surface, where the approximation of an irrotational acoustic field (i.e. $\nabla \times \vec{u}_1 = 0$) is generally valid. The term $\vec{S}_E$, however, will have a nonzero value in the medium away from the surface. Further support for this terminology lies in the observation that $\vec{S}_E$ is a function of the bulk viscosity; $\vec{S}_R$ and $\vec{S}_T$ are not.

Solutions to problems (A) and (B) mentioned above clearly indicate that in these two cases the surface sources of vorticity dominate the streaming. The flow velocity caused by the surface sources of vorticity is many orders of magnitude greater than that caused by the volume sources for these two cases. Although it has been suggested by Eckart[1] that the source $\nabla\rho_1 \times \nabla \partial\rho_1/\partial t$ might explain the streaming at the mouth of the Helmholtz resonator, the results of Schuster and Matz for a standing wave, and the author's calculations for a

traveling wave which fills a tube seem to imply otherwise. Possibly the theoretical solution to the problem of streaming at an orifice in a plate which blocks a standing wave in a tube[6] is also determined by the surface sources of vorticity. In general, the final assignment of the importance of the source terms can be made only after an evaluation of the terms of Eq. (5) through a knowledge of the actual first-order acoustic field. The difficulty of solving Eq. (5) for any but the simplest acoustic field and the simplest geometry is obvious.

II. STREAMING CAUSED BY A SOUND BEAM IN A CLOSED TUBE

The analysis of the preceding section provides a convenient breakdown of vortex streaming phenomena in tubes as due to surface sources of vorticity which predominate in a guided acoustic wave or volume sources which are most important in an acoustic beam. Obviously, the latter problem is of more interest since, as pointed out by Eckart, it appears to offer a direct approach to the determination of bulk viscosities. It seemed to the author that, preliminary to the use of the streaming equations developed by Eckart for this purpose, a complete survey should be made to study:

a) the variation of streaming with the pressure amplitude and distribution of the acoustic field, and

b) the variation of streaming with the medium.

The dependence of streaming on distribution of acoustic pressure could be studied in any medium. Then the use of a monatomic gas such as argon, with known values of bulk viscosity (zero), shear viscosity, and heat conductivity, serves to "calibrate" the experiment, so that the constant "b" may be determined and interpreted for other media.

To accomplish these goals, it is necessary to know the absolute values of the acoustic pressures and the absolute values of the streaming velocities at all points over a cross-section of a tube filled with a gas of known purity. The equipment used is described in section II-A. The extension of streaming theory based on the observed field

and comparison of predicted streaming velocities with observation is taken up in section II-B. Determination of bulk viscosities of moist air and dry nitrogen after calibration with argon is discussed in section II-C.

A. EQUIPMENT AND EXPERIMENTAL PROCEDURES

The ultrasonic streaming tube used was a glass pipe of six inches diameter and four foot length. The movable source holder at one end of the tube held a barium titanate disk transducer. The tube was terminated by a movable, glass-wool covered end piece. The over-all appearance is shown in Figure 1.

The source was a one-half inch thick, three inch diameter disk of pre-polarized barium titanate ceramic. It was supported at three points in its median plane and was capable of being driven in any of several modes between the frequencies 150 KC and 210 KC. Since the theoretical solution is based on the assumption of a radially symmetric field, this was checked first by sprinkling Lycopodium powder over the disk during vibration. The pattern observed for the mode selected for this experiment is shown at the top of Figure 2. This motion, which is not a piston-type mode, corresponds to a frequency of 185 KC.

Having determined that the source pattern of vibration was radially symmetric, it was then necessary to make the crystal axis colinear with the tube axis. An optical method was used. A small plane-parallel-faced mirror was pressed against the radiating face of the barium titanate. Then, sighting through a set of illuminated

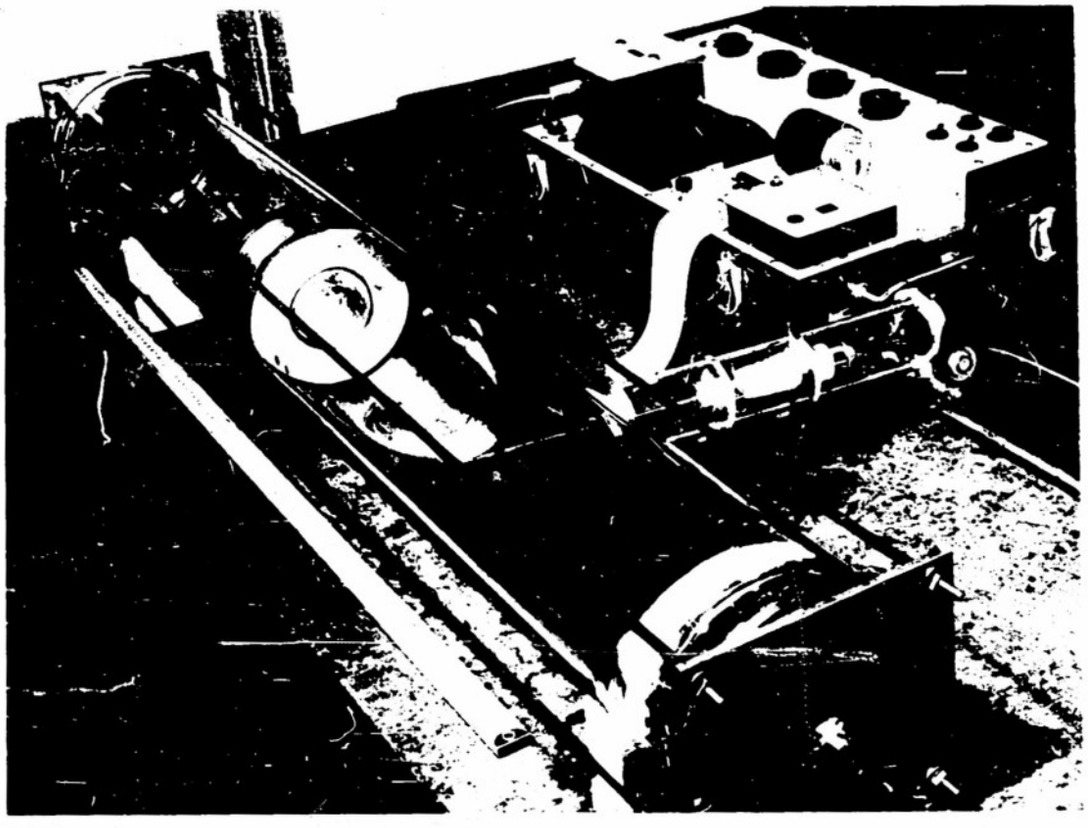

ACOUSTIC STREAMING TUBE

LEFT : Ba Ti O_3 source

RIGHT: Glass wool absorber

CENTER: A.D.P. Probe microphone and preamp. with recorder and drive

FIG. 1

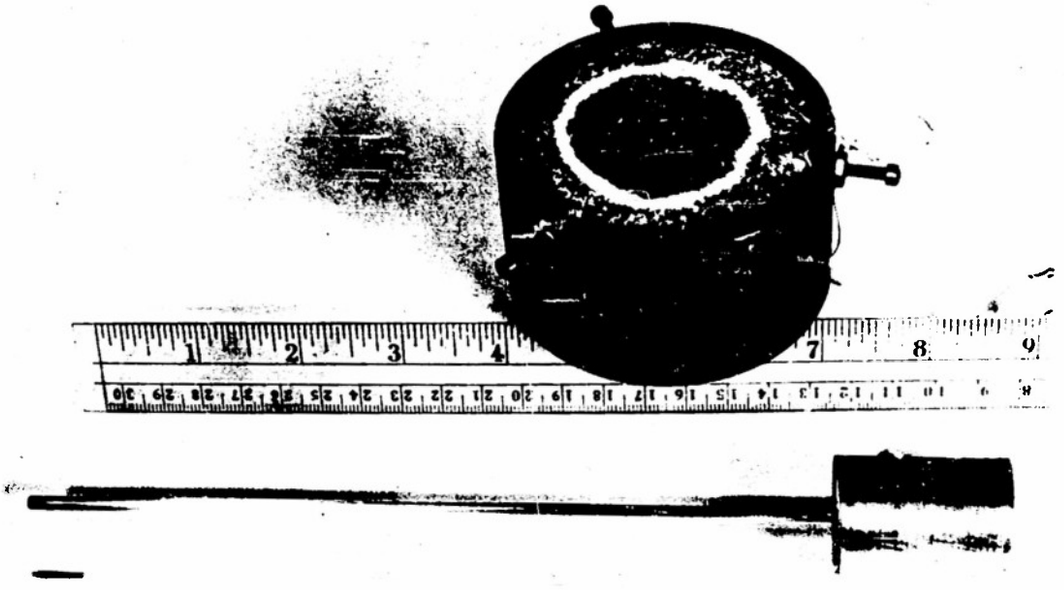

TOP: Lycopodium pattern of source

BOTTOM: Probe microphone with A.D.P. crystal at lower left

FIG. 2

cross-hairs centered on the axis and at the other end of the tube, the crystal was adjusted until the original cross-hairs and their image in the mirror were superimposed at the center of the mirror. Estimates of errors lead to the conclusion that this simplified Gaussian eyepiece technique would give a maximum angle of deviation of 15 minutes between the perpendicular to the crystal face and the tube axis. This amounts to the center of the beam being off-axis by a maximum of slightly over one millimeter for the conditions used in most of the experiment. That the radially-symmetric source vibrations gave a radially-symmetric acoustic field when aligned as described, is shown by the field recordings in Figure 3. The method of obtaining these records is described below.

Two, 1/8th inch O.D. probe microphones (lower object of Figure 2) were used, one mounted transverse to the tube on twin guide rails with rack and pinion drive, the other mounted through the end plate, with probe axis parallel to the tube axis. The transverse microphone was driven by the motor of a Bruel and Kjaer Recorder and was used to probe the acoustic field along a diameter. Different diameters could be probed by rotating the source holder about its own axis. Records for four of these diameters at a distance of 50 cm. from the source are superimposed in Figure 3. These records show the essentially radially-symmetric character of the field. The end microphone was used to monitor the acoustic field during streaming velocity observations when the transverse microphone was withdrawn. The sensitive element for each microphone was an ammonium dihydrogen phosphate (A.D.P.) longitudinal, 45° expander bar, approximately 0.8 mm. x 2 mm.

Linear Plots of Acoustic Pressure, $P_1(r)$, Along Four Diameters through Sound Beam, 50cm. from source.

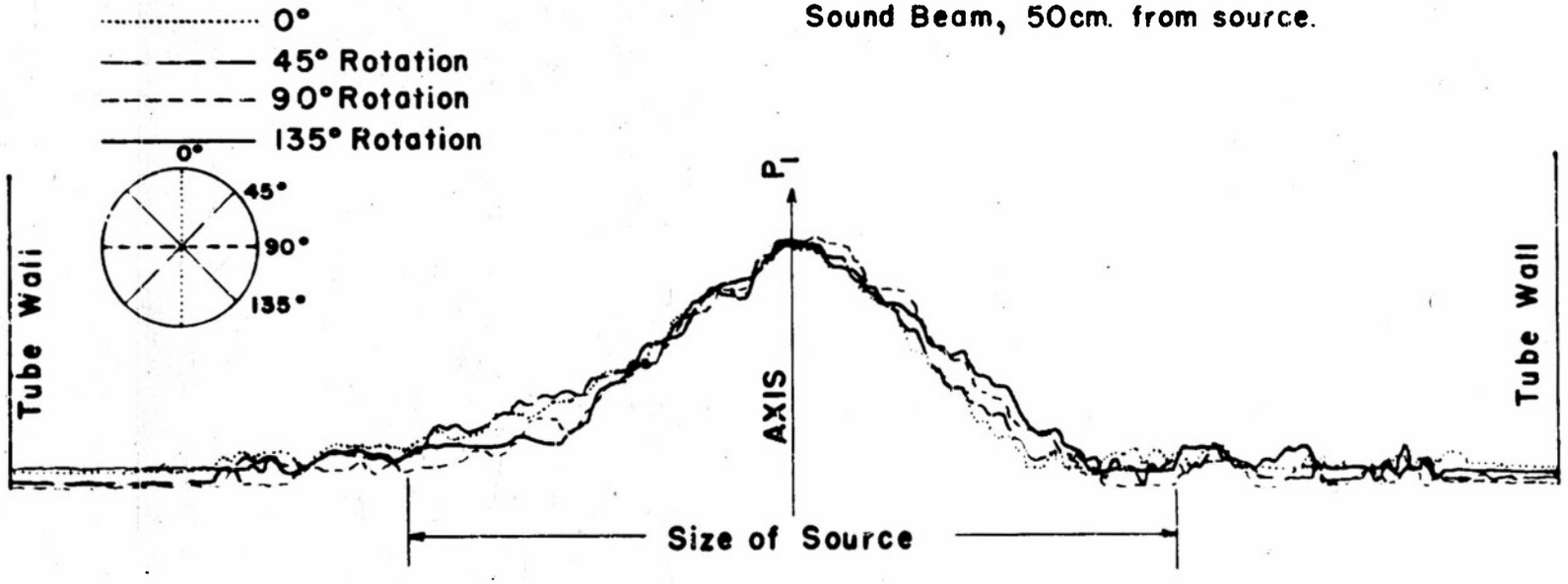

Fig. 3

x 7 mm. (see bottom-left corner of Figure 2) held at its midpoint so as to protrude slightly from the probe tube. A double shielded cable connected the crystal to a preamplifier adaptor. The sensitivity of the microphones was determined by direct comparison with a W.E. 640AA condenser microphone which was calibrated by reciprocity to an accuracy of $\pm$ 0.3 db.

Thermal convection proved to be a most troublesome interference. To minimize such deleterious effects it was necessary to place the streaming tube in the small U.C.L.A. anechoic chamber, which is in turn within a temperature controlled ($\pm$ 1°C.) room. Since body heat, itself, caused thermal streaming, motion of tobacco smoke or Lycopodium tracing particles was observed by telescope through a hole in the wall of the anechoic chamber. Line illumination of the particles in the tube was provided by a line filament lamp with spherical lens which gave a line image at a distance of about one foot from the light source. An infra-red filter was effective if the light was not used for more than 30 minutes at a time. Heating of the pre-amplifier and the probe microphone placed a 15 minute operation limit on the microphone. Heating of the source transducer imposed the most severe restriction on the experiment. After only three minutes the source would be warm enough to drive thermal convection streams for hours.

The telescope was provided with a reticle which was then calibrated for fields of view at various distances. In operation, the position of the illuminated line was set by moving the light source holder by means of its support rod which extended outside the anechoic chamber. The telescope was then focused on the particles which were

illuminated by the light, and a stop clock which read to hundredths of seconds was used to time the passage of the particles past a calibrated reticle distance.

The electronic circuitry is shown in the block diagram of Figure 4. The barium titanate transducer was driven by a signal from a G.R. 716A oscillator, whose output was amplified by the amplifier section of a W.E. 17B oscillator. The microphones were adapted to the Western Electro-Acoustic Pre-amplifier and Microphone Complement 100b, with bias voltages blocked from the A.D.P. crystals. The output of the Complement was sent through a Navy RAK 7 receiver for amplification and filtering. This output was applied to the voltmeter or to the Bruel and Kjaer recorder.

The rather complex source holder shown in Figure 1 was necessary to provide for air-tight movement in the (unfortunately) slightly tapered glass tube. Since all experiments were carried on at atmospheric pressure, only diffusion at no difference of pressure could bring in impurities. To minimize such leaks, "O" rings were used throughout. The source holder slides on two "O" rings which are kept tight by twelve bolts passing through their own "O" rings. Tightening the bolts squeezed the large "O" rings out to contact the variable I.D. tube. The microphone probes also passed through "O" rings. One-quarter inch steel end plates supported the 450 pound force of air pressure exerted on the source holder and end piece during evacuation for change of gas. The equivalent leakage area was calculated to be 10^{-2} mm^2 by the change of pressure as air seeped into the tube after evacuation. Diffusion through such an area would give only about

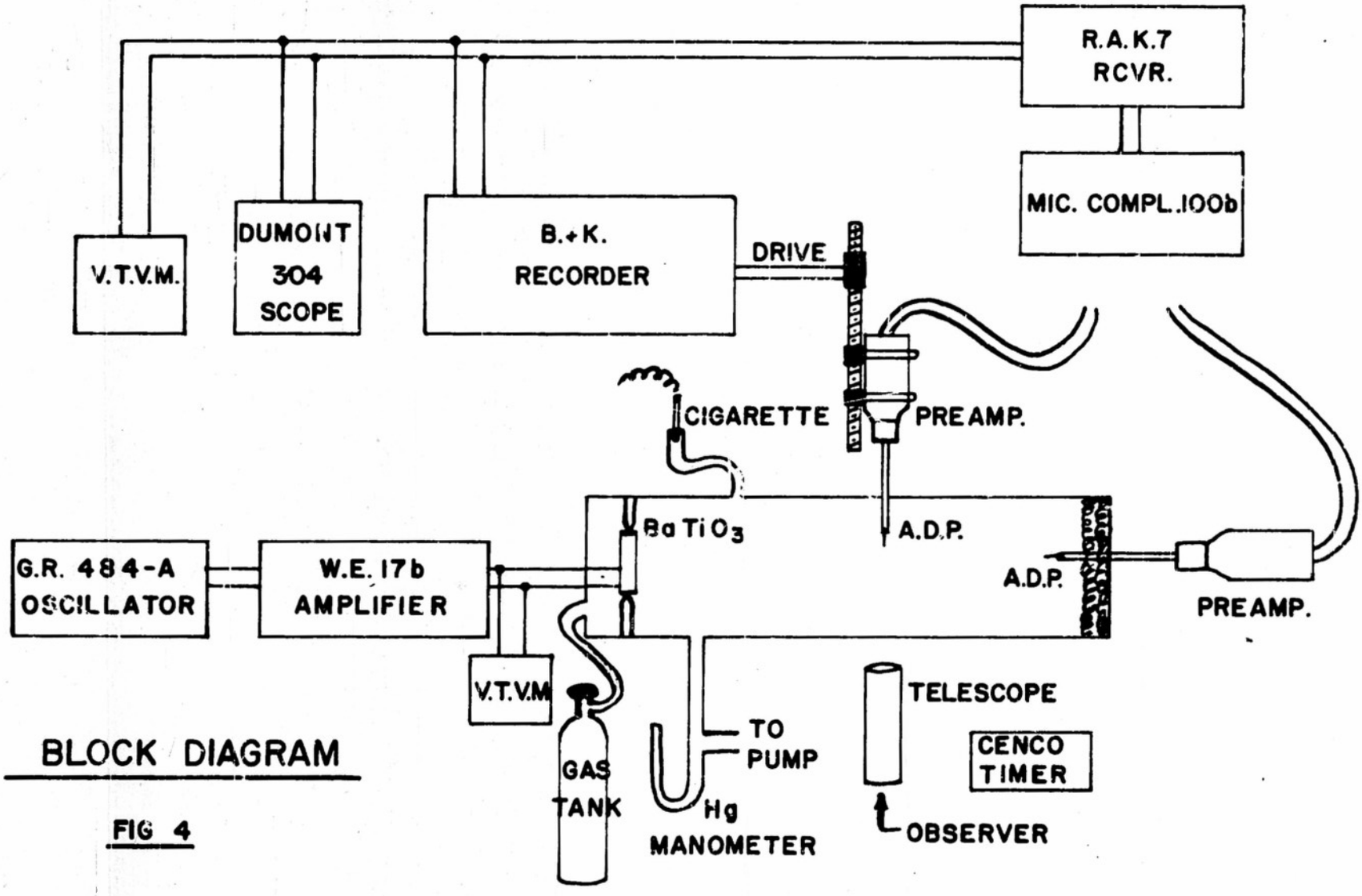

BLOCK DIAGRAM

FIG 4

0.01% impurity in 100. hours. No gas sample was ever kept in the tube for more than 24 hours in the experiment.

The gases used in the experiment were moist laboratory air, commercial argon, and commercial, oil-pumped nitrogen. The nitrogen was asserted, by the supplier, to be 99.7% pure with 0.01% water molecules. Both Lycopodium powder and tobacco smoke were used as tracing particles, with no real difference in the streaming observed. It is felt that the water molecule impurity was no more than 0.03% and had no measurable effect on the streaming in nitrogen or argon.

B. DEPENDENCE OF STREAMING ON ACOUSTIC FIELD

Using only the first term of equation (5), Eckart shows that a radially-symmetric progressive sound beam of acoustic pressure,

$$P_1 = \rho_1 c_o^2 = P(r) \sin (kZ - wt)$$

in a tube of radius r_o, will cause streams which have a distribution with r given by:

$$u_2(r) = K \int_o^{r_o} \Gamma(s,r) P^2(s) ds + \beta(r_o^2 - r^2) \qquad (7)$$

where $K = (\frac{1}{2} bk^2)/(\rho_o^2 c_o^3)$

$k = 2\pi/\lambda$

$\omega = 2\pi f$

ρ_o = static fluid density

c_o = speed of sound

$b = 4/3 + \mu'_o/\mu_o$

$$\Gamma(s,r) = s \log (r_o/r) \quad \text{when } s \leq r \qquad (8)$$

$$= s \log (r_o/s) \quad \text{when } s \geq r$$

$$\beta = -(K/r_o^4) \int_o^{r_o} (rr_o^2 - r^3) P^2(r) dr \qquad (9)$$

The applicability of these equations to a real acoustic field in air has been experimentally studied by the author with regard to;

1) variation of streaming with acoustic intensity,
2) variation of streaming (both on axis and off) with acoustic field distribution, and
3) attenuation of axial stream velocity near a source of sound.

1) Variation of Streaming with Acoustic Field Intensity

Equations 7-9 predict that the streaming velocity should be proportional to the square of the acoustic pressure at a point (for a fixed field distribution). It is necessary to investigate this functional dependence for the range of intensities to be studied before using the theory.

Observation of tobacco smoke or Lycopodium powder tracing particles was used throughout the experiment and gave accurate values up to speeds of about 1.3 cm/sec. Within the range up tc 1.3 cm/sec, u_2 is apparently proportional to p_1^2. This is shown in Figure 5.

This result may be compared with two criteria which have appeared in the literature. First, for direct current flow in a smooth pipe, the critical Reynold's Number, $R_c = u_2 d/\nu$, at which turbulence sets in is 2000 or greater depending on entry conditions of the stream.[7] Such a criterion applied to this experiment would predict onset of non-linearity at a flow velocity of 200 cm/sec. On the other hand, Liebermann[8] has conducted an experiment similar to this one (but

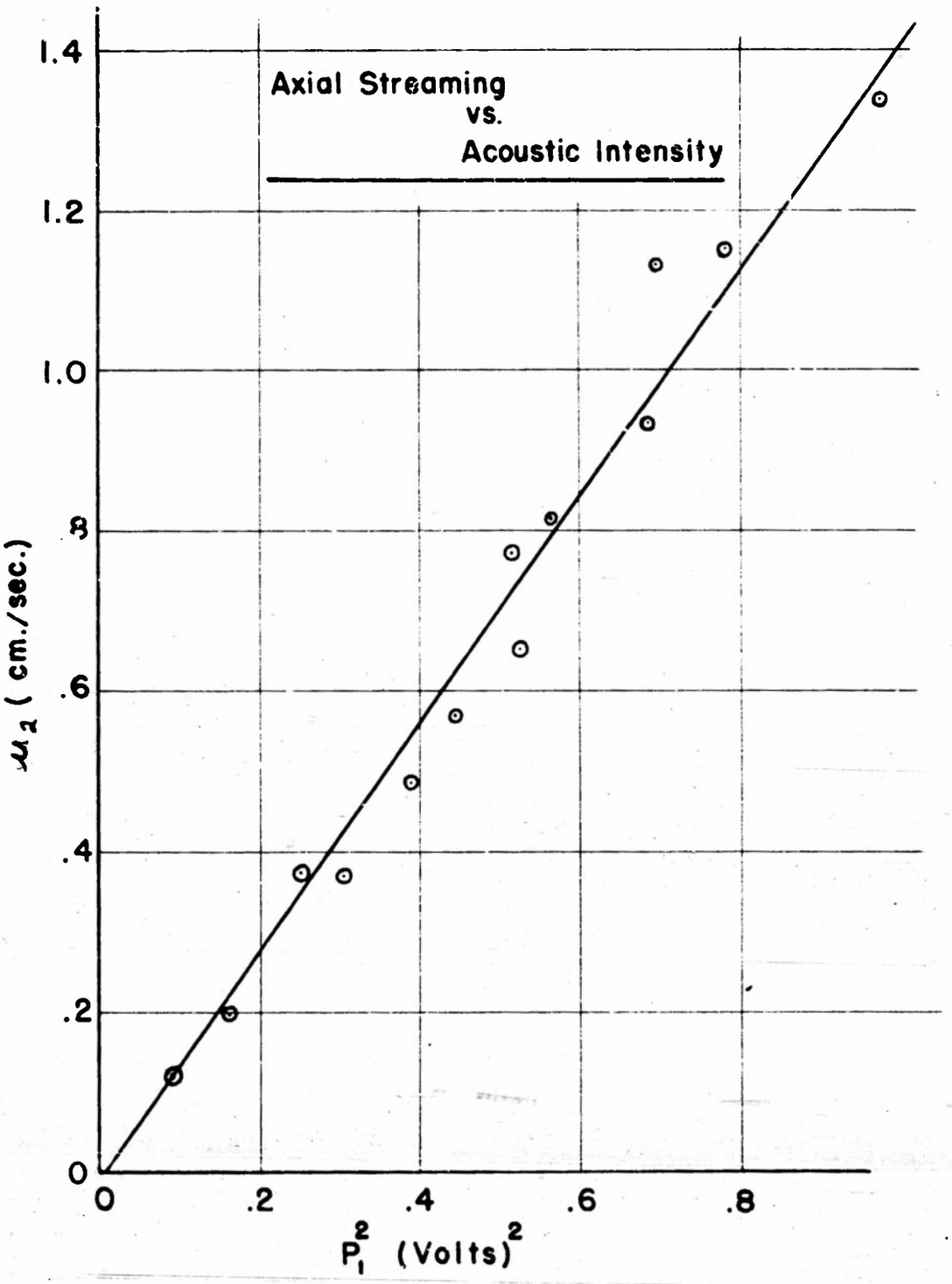
Axial Streaming
vs.
Acoustic Intensity
1.4
1.2
1.0
.8
.6
.4
.2
0
u_2 (cm./sec.)
0
.2
.4
.6
.8
P_1^2 (Volts)^2

FIG. 5

in liquids) and found that the constant of proportionality between u_2 and p_1^2 changed at a Reynold's Number of about 20. If this criterion held here, non-linearity would be expected at velocities greater than $u_2 \tilde{-} 2$ cm/sec. No such change of linearity was observed in the range of axial velocities from zero to 1.3 cm/sec.

2) Variation of Streaming with Acoustic Field Distribution

If, for simplicity, one assumes an "ideal" acoustic beam given by

$$P_1(r) = P_{10} \quad , \quad r \leq r_1 \qquad (10)$$
$$P_1(r) = 0 \quad , \quad r > r_1$$

where r_1 is the radius of the non-divergent sound beam, there results from equations (7)-(10) a prediction of an axial stream velocity, for such an "ideal" field:

$$u_2(0) = \tfrac{1}{2} K P_{10}^2 r_1^2 \left\{ \frac{r_1^2/r_o^2 - 1}{2} - \log r_1/r_o \right\}$$

$$= \frac{\omega^2 r_1^2 G I}{2\rho_o c_o^4} \, b \qquad (11)$$

where $G = (r_1^2/r_o^2 - 1)/2 - \log r_1/r_o$

$b = 4/3 + \nu'/\nu$

$I = P_{10}^2/(2\rho_o c_o)$

This last equation was derived by Eckart and used by Liebermann. Liebermann's velocities were obtained by measurements of force on a diaphragm which had been calibrated by observation of tracing particles moving with the fluid.

When a probe microphone is used to determine the actual distribution of acoustic pressure in the field, it is possible to substitute this information into equations (7)-(9) and, thereby, to get a more realistic prediction of the streaming. Without question, the actual

field $P_1(r)$ should be used to calculate the streaming, and this is what has been done in these experiments. However, it is of interest to compare the axial streaming predicted by the actual field with the streaming predicted when one uses the "ideal" field assumption. It will be proved that a gross error would be made in the streaming prediction if one replaced the actual field used in this experiment by an equivalent-energy, "ideal," field as described by equation (10).

a. Axial Velocity

For the special position r = 0, but with the general field distribution, P(s),

$$s \geq r \qquad \text{and} \qquad \Gamma(s,r) = s \log r_o/s.$$

Then,

$$u_2(0) = K\int_o^{r_o} s \log (r_o/s)\, P^2(s) - K/r_o^2 \int_o^{r_o} (sr_o^2 - s^3)P^2(s)ds$$

$$= K\int_o^{r_o} Q\, P^2(r)\, dr \qquad (12)$$

$$\text{where } Q = r \log(r_o/r) - r + r^3/r_o^2$$

Q(r) is a "weighting" factor which determines the contribution to the axial velocity, of the quantity $P^2(r)$. Figure 6 is a plot of $Q(r)/r_o$ vs. r/r_o and emphasizes the fact that it is the distribution of $P^2(r)$ which is significant in determining both the streaming speed and direction on the axis. (Note: A tubular field with a "hole" on the axis, would result in axial streaming opposite to the direction of propagation of the sound beam.)

In the following discussion, P_{1C} will be used to designate the axial (r = 0) maximum value of the acoustic pressure. The measurements at 72 cm from the source are considered first, and the axial maximum acoustic pressure at this point is designated by P_{107}. Figure

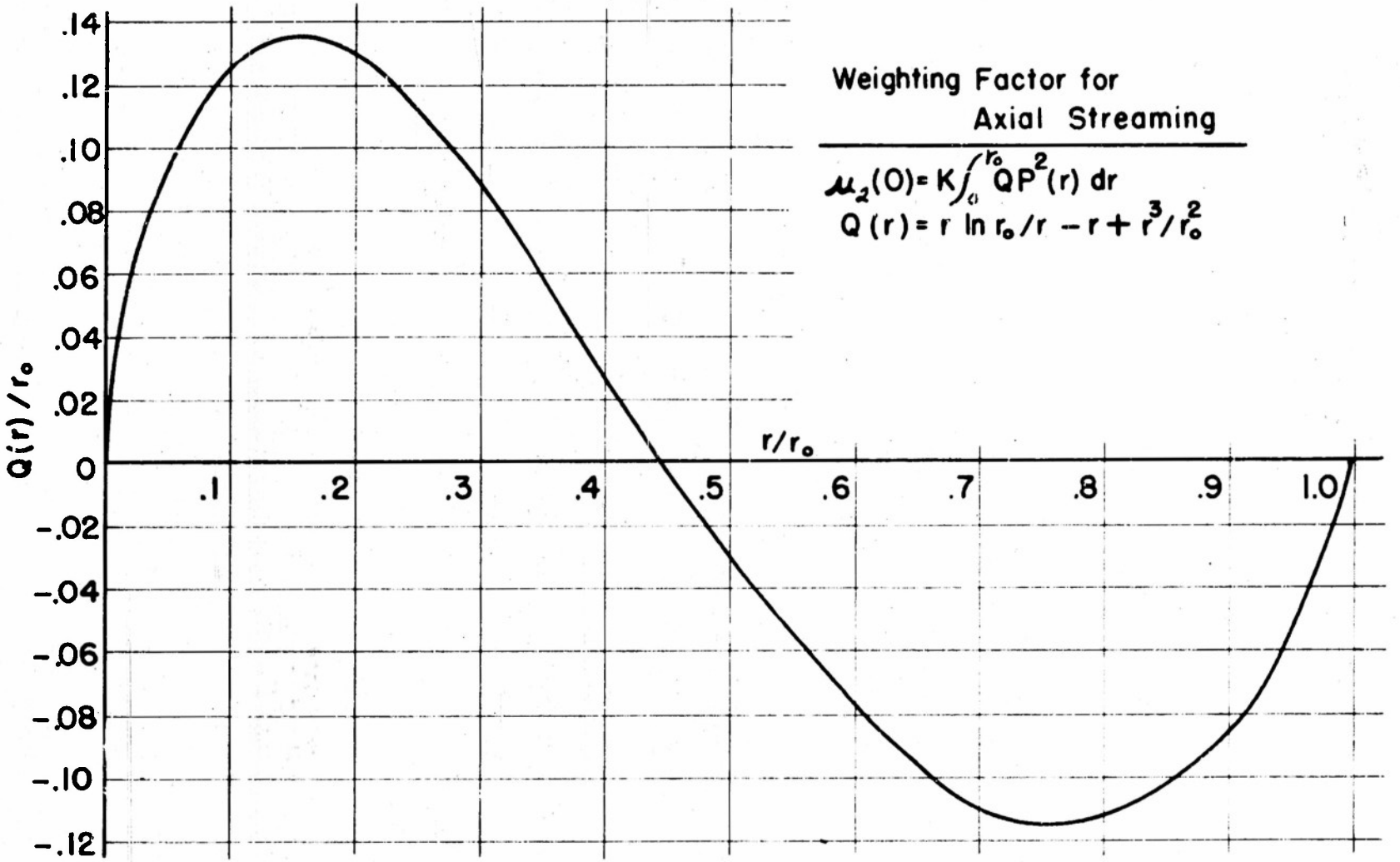
Weighting Factor for
Axial Streaming
$\mu_2(0) = K \int_0^{r_o} QP^2(r)\, dr$
$Q(r) = r \ln r_o/r - r + r^3/r_o^2$
Q(r)/r₀
r/r₀
.14
.12
.10
.08
.06
.04
.02
0
-.02
-.04
-.06
-.08
-.10
-.12
.1
.2
.3
.4
.5
.6
.7
.8
.9
1.0

FIG. 6

7 shows the average (or all eight radial probings) pressure $P(r)$, $P^2(r)$ and $rP^2(r)$.

The stream velocity at the axis, u_{20}, is obtained by a graphical integration of $QP^2(r)dr$, performed in Figure 8. This evaluation gives:

$$u_{207} = K\int_o^{r_o} QP^2(r)dr = 0.0180\, KP_{107}^2\, r_o^2 \qquad (13)$$

It remains to answer the question, "What axial streaming is predicted if one assumes an 'ideal field' of maximum pressure $\sqrt{\overline{P^2}}$, where $\overline{P^2}$ is defined so that the force of its radiation pressure against a hypothetical end diaphragm equals that caused by the actual field?" For both fields to exert the same force on a diaphragm:

$$(\pi r_1^2)\left(\frac{\overline{P^2}}{2\rho_o c_o^2}\right) = \frac{2\pi}{2\rho_o c_o^2}\int_o^{r_o}\left[P_1(r)\right]^2 r\, dr$$

$$\overline{P^2} = 2/r_1^2\int_o^{r_o}\left[P_1(r)\right]^2 r\, dr = 8/r_o^2\int_o^{r_o} r\left[P_1(r)\right]^2 dr$$

where r_1 = "ideal" beam radius = $r_o/2$

As defined, this mean square pressure, $\overline{P^2}$, is assumed to have the above, constant, value over a "measurement circle" equal to the source area, and the radiation pressure is zero everywhere else.

The graphical integration is performed in Figure 7 and yields

$$\int_o^{r_o} rP^2(r)\, dr = 0.0268\, r_o^2\, P_{107}^2$$

$$\overline{P^2} = (8/r_o^2)(.0268 r_o^2 P_{10}^2) = 0.214\, P_{107}^2$$

$$u_{207} = K\int_o^{r_o} Q\ \overline{P^2}\, dr = 0.214KP_{107}^2\int_o^{r_1} Q dr$$

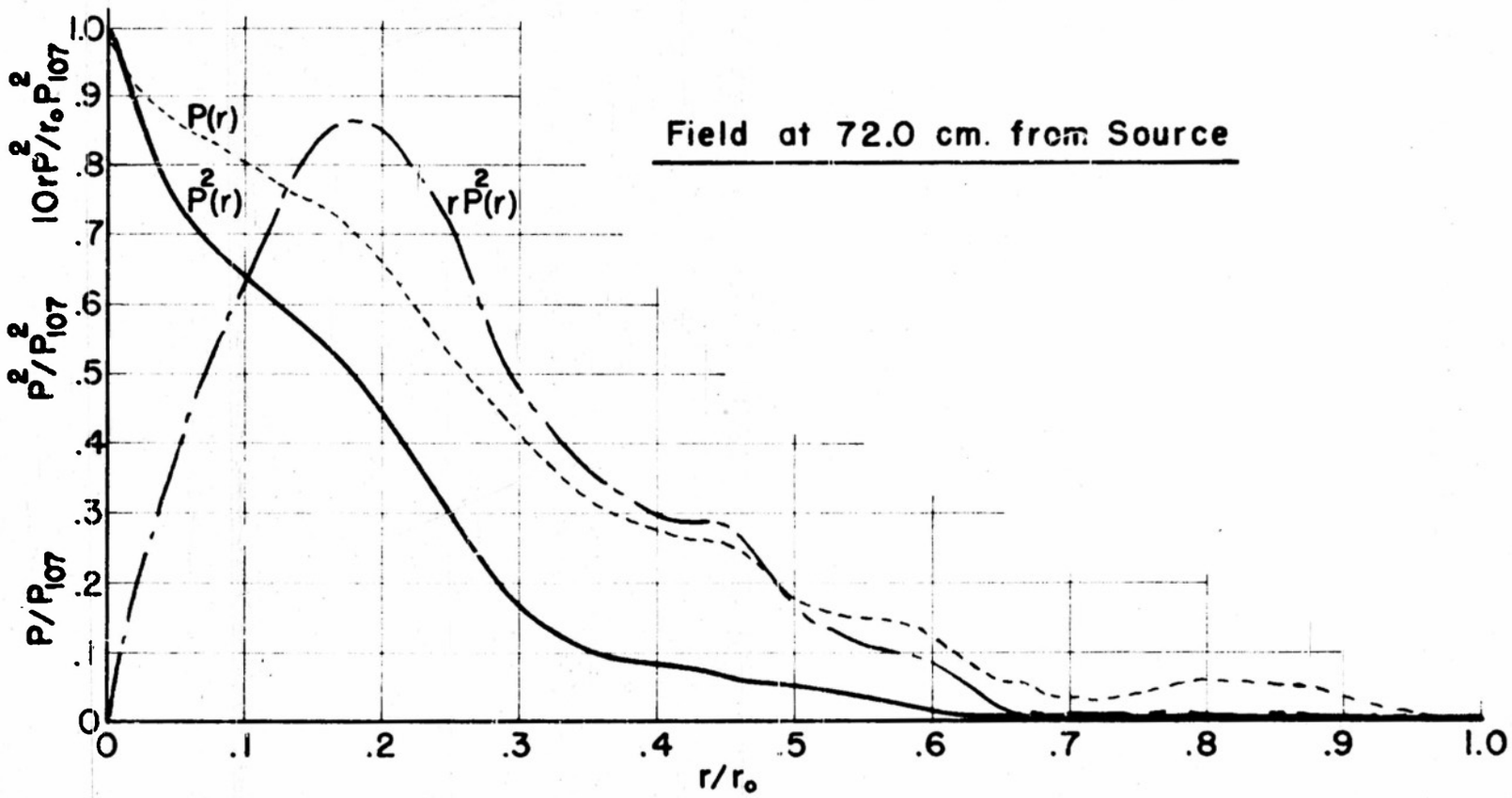
Field at 72.0 cm. from Source
P(r)
P²(r)
rP²(r)
10rP²/r₀P₁₀₇²
P²/P₁₀₇²
P/P₁₀₇
r/r₀
0
.1
.2
.3
.4
.5
.6
.7
.8
.9
1.0

FIG. 7

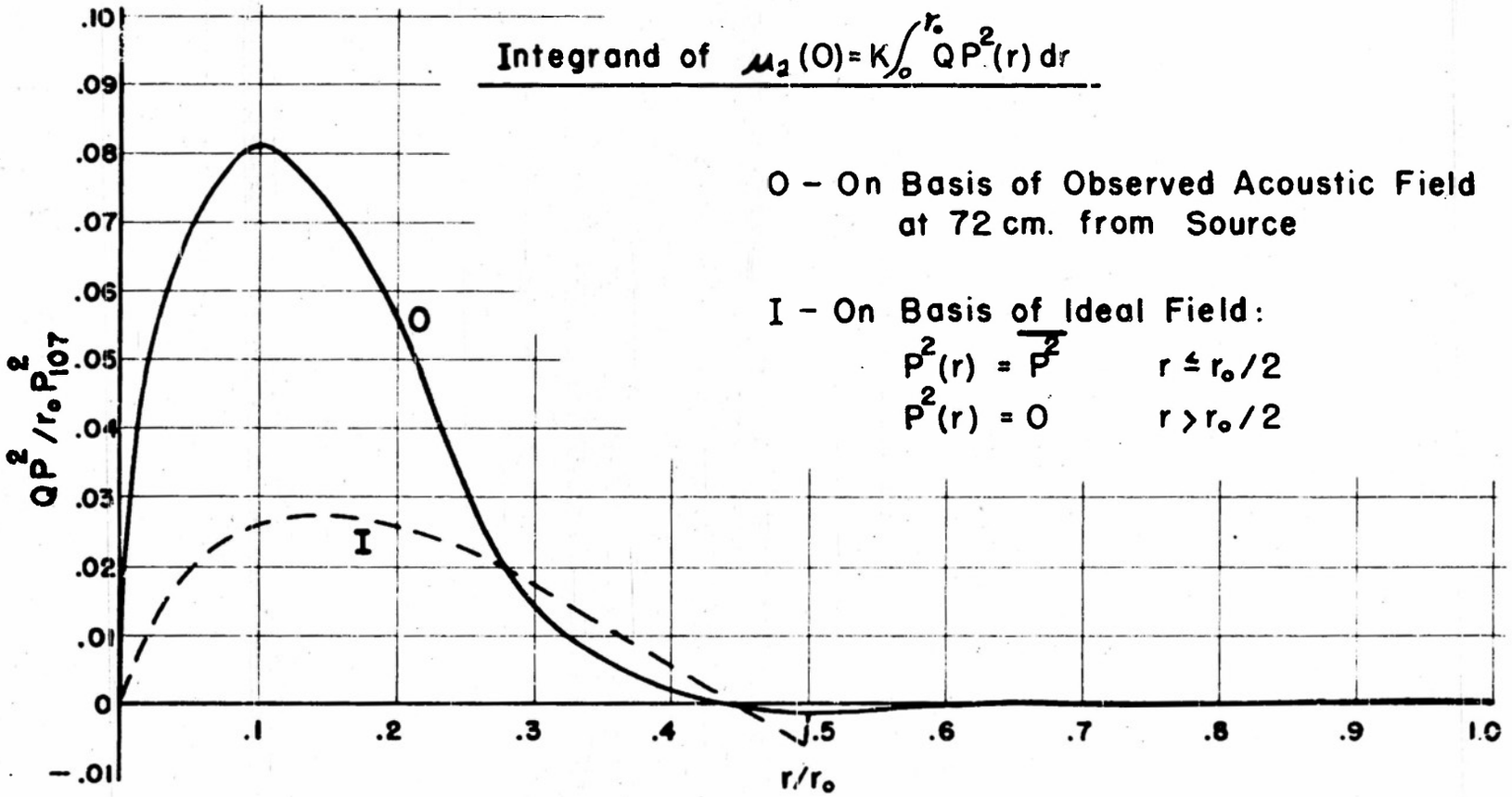
Integrand of $\mu_2(0) = K\int_0^{r_0} Q P^2(r)\, dr$
O – On Basis of Observed Acoustic Field at 72 cm. from Source
I – On Basis of Ideal Field:
$P^2(r) = \overline{P^2}$ $r \leq r_0/2$
$P^2(r) = 0$ $r > r_0/2$
$QP^2/r_0P_{107}^2$
.10
.09
.08
.07
.06
.05
.04
.03
.02
.01
0
-.01
O
I
.1
.2
.3
.4
.5
.6
.7
.8
.9
1.0
r/r_0

FIG. 8

Finally, $$u_{207} = 0.0085\, KP_{107}^2 r_o^2 \qquad (14)$$

Comparing equations (13) and (14), it is clear that the axial streaming velocity predicted by the actual acoustic field is 2.12 times as great as the value obtained on the basis of an equivalent "ideal" field. Otherwise stated, if the axial velocity was observed and then used in equation (11) to solve for the value of b, the value of b so obtained would be approximately twice the correct value.

b. Off-axis Velocities

Not only the magnitudes, but also the streaming profile (the variation of streaming with distance from axis), is altered when the actual field rather than the ideal field is used in the theory. The method used to get an analytic expression for the streaming velocity, $u_2(r)$, was to approximate the acoustic field P(r) by three straight line regions defined by:

$$\begin{aligned} &\text{Region A,} && P(r) = P_{10}(ar/r_o + b) && \text{for } 0 < r \leq r_2 \\ &\text{Region B,} && P(r) = P_{10}(cr/r_o + d) && \text{for } r_2 \leq r \leq r_3 \\ &\text{Region C,} && P(r) = 0 && \text{for } r \geq r_3 \end{aligned} \qquad (15)$$

For such a field, equations (7), (8) and (9) provide the analytic expressions:

$$\begin{aligned} u_2(r) = {} & \overbrace{KP_{10}^2 r_o \{\log y\,[\, y^4/4(c^2-a^2) + 2/3y^3(cd-ab) + y^2/2(d^2-b^2)\,]}^{0<r<r_2} \\ & -\log z(c^2z^4/4+2/3\, cdz^3+d^2/_2z^2) + a^2/16(y^4-x^4) + 2/9ab(y^3-x^3) \\ & + b^2/4\,(y^2-x^2) + c^2/16(z^4-y^4) + 2/9cd(z^3-y^3) + d^4/4(z^2-y^2)\,\} \\ & + \beta r_o^2(1-x^2) \end{aligned}$$

$$\begin{aligned} u_2(r) = {} & K\, P_{10}^2\, r_o^2 \{-\log x[y^4/4(a^2-c^2) + 2/3y^3(ab-cd) + y^2/2(b^2-d^2)\,] \\ & \overbrace{-\log z[z^4/4\, c^2+2/3z^3cd+d^2/2\, z^2] + c^2/16(z^4-x^4) + 2/9cd(z^3-x^3)}^{r_2\leq r\leq r_3} \\ & +d^2/4(z^2-x^2)\} + \beta r_o^2(1-x^2) \end{aligned}$$

$$\begin{aligned} u_2(r) = {} & -KP_{10}^2 r_o^2 \log x[\, y^4/4(a^2-c^2) + 2/3y^3(ab-cd) + y^2/2(b^2-d^2) + c^2/4z^4 \\ & \overbrace{+ 2/3cdy^3 + d^2/2z^2]}^{r\geq r_3} + \beta\,(r_o^2-r^2) \end{aligned} \qquad (16)$$

$$\begin{aligned} \beta = {} & -KP_{10}^2\,\{-z^6c^2/6 + y^6/6(-a^2+c^2) - 2/5z^5cd + 2/5y^5(cd-ab) + z^4/4(c^2-d^2) \\ & + y^4/4(a^2-b^2-c^2+d^2) + 2/3z^3cd + 2/3y^3(ab-cd) + d^2z^2/2 + y^2/2(b^2-d^2)\} \end{aligned}$$

where $x = r/r_o$, $y = r_2/r_o$ and $z = r_3/r_o$

The average observed pressure distributions, as well as the straight line approximations, are shown in Figure 9 for three distances from the source. From these, the following numerical values were taken for the two cases, 26 cm from the source and 72 cm from the source:

	Distance from Source	
constant	72 cm	26 cm
a	-1.820	-3.480
b	1.000	1.000
c	-0.770	-0.372
d	0.580	0.223
y	0.400	0.250
z	0.750	0.600

Use of these constants in equation (16) then gives values of $u_2(r)$ from which the curves of Figure 10 are drawn for the streaming profiles at 26 cm and 72 cm from the source. The streaming predicted by the "ideal" field approximation (for beam radius $r_1 = r_o/2$) is also shown in Figure 10.

All three curves are plotted with the same axial velocity to aid in comparing the profiles. It must be remembered that the actual field method would give streaming magnitudes different than those obtained from the equivalent "ideal" field approximation. More will be said about this in the next section. As a check on the ability of equations (15) to take the place of the actual field, the axial velocity (for 72 cm from the source) obtained here is $0.0184\ K_{107}^2 r_o^2$ as compared to $0.0180\ K_{107}^2 r_o^2$, obtained by use of formula (13). Figure 10 shows that the stream velocity may be expected to drop off

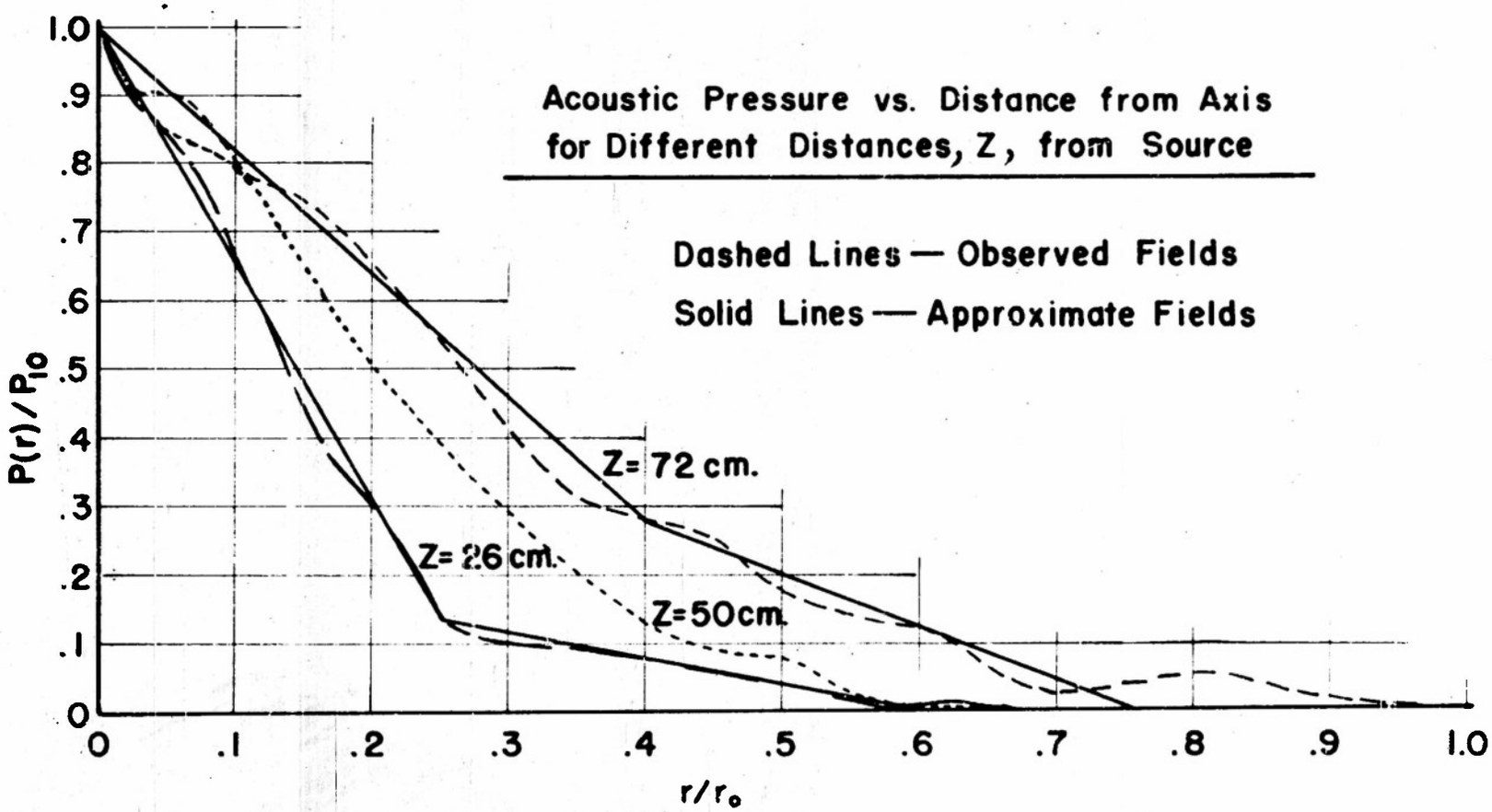
Acoustic Pressure vs. Distance from Axis
for Different Distances, Z, from Source
Dashed Lines — Observed Fields
Solid Lines — Approximate Fields
Z= 72 cm.
Z= 26 cm.
Z=50cm.
P(r) / P10
r/r0
1.0
.9
.8
.7
.6
.5
.4
.3
.2
.1
0
0
.1
.2
.3
.4
.5
.6
.7
.8
.9
1.0

FIG. 9

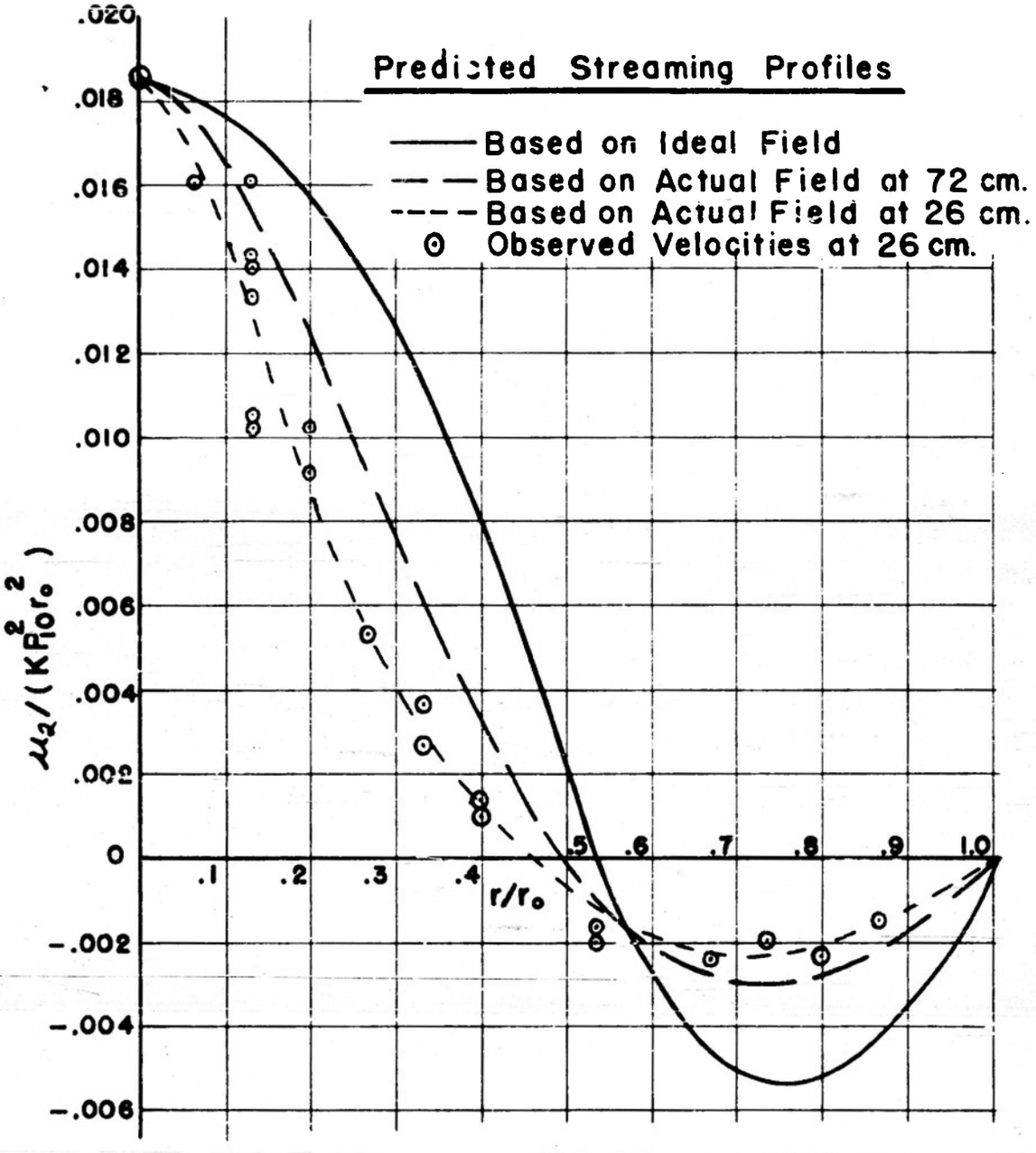
Predicted Streaming Profiles
Based on Ideal Field
Based on Actual Field at 72 cm.
Based on Actual Field at 26 cm.
Observed Velocities at 26 cm.
.020
.018
.016
.014
.012
.010
.008
.006
.004
.002
0
-.002
-.004
-.006
.1
.2
.3
.4
.5
.6
.7
.8
.9
1.0
r/r₀
u₂/(KR₁₀²r₀²)

FIG. 10

from the axial value more rapidly, that the change in direction occurs nearer to the axis, and that the counter-flow is relatively slower, than for the "ideal" field. These differences are greater at 26 cm than at 72 cm from the source.

The plotted points in Figure 10 are experimental values of the streaming at 26 cm from the source. The spread in the values at $r/r_o = 0.133$ may be explained by an error of only 2 mm in positioning of the light source. It may be said that when the observed acoustic field is used to predict the streaming velocity profile a very good check with experiment is obtained.

3) Quantitative Verification of Stream Velocity Prediction

It remains to check the magnitude of the streaming velocity by study of a gas, such as argon, of known physical constants. The interpretation of the cause of acoustic streaming is tied up in the constant b of equation (11). As used by Eckart, $b = 4/3 + \mu'/\mu$, but Eckart did not consider thermal conductivity or relaxation processes, as such. More recently, Markham[9] has extended the streaming theory to consider the effect of relaxation processes.

Instead of using the realtion, $p_1 = \rho_1 c_o^2$, one takes account of the possibility of acoustic pressure depending on the rate of change of density by expressing

$$p_1 = c_o^2 \rho_1 + \mathcal{R}\dot{\rho}_1 \qquad (17)$$

where the dot indicates differentiation with respect to time, and where $\mathcal{R}$ is some kind of relaxation constant.

The first-order equation (3) becomes

$$\rho_o \frac{\partial \vec{u}_1}{\partial t} = - C_o^2 \nabla \rho_1 - \mathcal{R} \nabla \dot{\rho}_1 + b \mu_o \nabla \nabla \cdot \vec{u}_1 - \mu_o \nabla \times \vec{R}_1$$

But since the equation of continuity (2a) is

$$\partial \rho_1 / \partial t + \rho_o \nabla \cdot \vec{u}_1 = 0 \qquad (2a)$$

it is possible to write

$$\rho_o \partial \vec{u}_1 / \partial t = - C_o^2 \nabla \rho_1 + \mathcal{R} \rho_o \nabla \nabla \cdot \vec{u}_1 + b \mu_o \nabla \nabla \cdot \vec{u}_1 - \mu_o \nabla \times \vec{R}_1 = - C_o^2 \nabla \rho_1 + b^* \mu_o \nabla \nabla \cdot \vec{u}_1 - \mu_o \nabla \times \vec{R}_1 \qquad (18)$$

where $b^* = b + \mathcal{R} \rho_o / \mu_o = 4/3 + \mu' / \mu_o + \mathcal{R} \rho_o / \mu_o$

The argument, which was first proposed in the literature by Fox and Herzfeld,[10] and has been strengthened by the work of Markham[9] and W. Nyborg,[11] is that the momentum of the streams is evidence of the conversion of acoustic momentum lost by the attenuated sound beam. According to this argument, the constant b^* in equation (18) incorporates all attenuative mechanisms. Actually, it has long been known that even shear viscosity and thermal conductivity may be considered as relaxation phenomena, the relaxation times being close to the time between molecular collisions. From this point of view, thermal conductivity may be included in b^* by writing

$$\mathcal{R} \rho = (\gamma - 1) \kappa / C_p$$

where γ = ratio of specific heats

κ = thermal conductivity

C_p = specific heat at constant pressure.

The logical conclusion of such an argument is that one may write

$$b^* = \frac{2\rho_o c_o \alpha}{k^2 \mu} = 4/3 + (\gamma - 1)\kappa/(\mu C_p) + \mu'/\mu \qquad (19)$$

where α = amplitude attenuation coefficient,
nepers per unit length
$k = 2\pi/\lambda$ = acoustic wave number,

and that the determination of b^* either through a streaming experiment or through attenuation measurements would give the same results.

In equation (19), it is clear that streaming is proportional to the attenuation and inversely proportional to the shear viscosity of the medium. That is, the streams are driven by the rate of loss of momentum from the acoustic wave, and are retarded by the shear viscosity (at the walls of the tube). The well-known classical mechanisms of shear viscosity and thermal conductivity have been separated out, in equation (19), and the quantity μ' now represents a bulk viscosity which presumably takes account of all intra-molecular processes, including molecular relaxation phenomena plus any "inherent" bulk viscosity (if there is any such quantity).

Both theory[12] and recent experiment[13] support the assumption that $\mu' = \nu' = 0$ for argon. The attenuation is definitely classical, and therefore one would expect the streaming to depend only on the classical mechanisms of shear viscosity and heat conductivity. The constants for argon are very well known, and substitution into equation (19) gives

$$b^*_{\text{argon}} = 2.25$$

The experimental, streaming, determination of b^* for argon was performed by observing the axial values P_{102} and u_{202} at 26 cm from

the source. Equations (25) and (26) of the next section are used to determine the geometrical constant of proportionality between P_{102} and u_{202}, which is

$$u_{202} = .00940\, KP_{102}^2\, r_o^2 = .00940\, \frac{b^* \omega^2 (P_{102}^2/2)\, r_o^2}{\rho_o^2\, C_o^5} \qquad (20)$$

The critical information needed for the evaluation of b^* for argon includes the calibration of the ADP microphone in argon. First a WE 640AA microphone was calibrated by free-field reciprocity at 185 KC in air to give

$$M_{640} = -97.9 \text{ db re 1 volt per dyne / cm}^2.$$

Then a flat (± 1 db) region of the field of the $BaTiO_3$ source was located and the 640AA and the transverse ADP alternately placed in this region to give the relative response. Taking account of the differences between the gains of the two pre-amplifiers, it was found that

$$M_{ADP} = M_{640} - 17.9 \text{ db}.$$

Finally, since the end of the ADP was approximately one-half wavelength in thickness, it was necessary to observe the difference in sensitivity of ADP in air vs. in argon. (The wave length in air is approximately 10% greater than in argon. The beam diffraction was experimentally found to be independent of this small difference in wavelength which was as expected. However, the relative size of microphone to wavelength made the microphone very sensitive to small changes in wavelength.) With the 640AA at the end of the tube to monitor the field intensity, change of medium from air to argon was accompanied by

a decrease in ADP sensitivity of 4.2 db. The resulting sensitivity of the ADP in argon was

$$M_{ADP,argon} = 120.0 \text{ db re 1 volt per dyne/cm}^2.$$

With the RAK7 amplification of 52.5 db and the Microphone Complement plus Pre-amplifier gain of 35.8 db, an output of 1 volt rms meant an ADP output of -88.3 db re 1 volt. This represents an acoustic field of 31.7 db above 1 dyne/cm^2, or an acoustic rms pressure of 38.5 dyne/cm^2. The accompanying streaming reduced to one volt output was 0.0268 cm/sec.* These values and the constants for argon give

$$b^* = (u_{202}) \frac{\rho_o^2 c_o^5}{0.00940\omega^2 r_o^2 (P_{102}^2/2} = 2.34$$

which differs from the classical or attenuation value of b^* by only 4%.

At this juncture it is worthwhile to restate the assumptions which were made in the theoretical solution, and which seem to be supported by this experimental check. These assumptions were:

1) that the Navier-Stokes equation, the equation of continuity and the acoustic equation of state $p_1 = \rho_1 c_o^2 + \mathcal{R}\dot{\rho}_1$ provide a valid basis for second-order studies of streaming;
2) that thermal conduction effects may be introduced into the Eckart streaming equations in the same manner as they appear in attenuation formulas;

and, more particularly in this experiment,

---

*This is the average of four separate series of observations (a total of twenty timings) using both Lycopodium and tobacco smoke as tracing particles, in two different gas samples. The maximum deviation of the four values from the mean value presented above was 6%.

3) that $\vec{S}_E$ was the only effective source of vorticity;

4) that the divergence, attenuation and departure from plane-wave character of this sound beam permitted the assumption

$$p_1 = p_1(r) \sin (kx - \omega t)$$

rather than the more accurate (and virtually unmanageable) description

$$p_1 = p_1(r,x)_e^{-\alpha x - j\omega t}$$

The validity of assumption 4) is discussed in Appendix B.

4) Attenuation of Axial Stream Velocity (Quartz Wind)

In the earlier explanations of the "quartz wind," the fluid flow was ascribed to an ill-defined, local rectifying action due to the vibrating crystal. It will be shown here that Eckart's theory, when properly applied to the actual acoustic field, gives a quantitative explanation of the observed decrease in axial streaming velocity as one recedes from the source.

The variation in axial stream velocity was observed at various distances from 20 cm to 72 cm from the source. Three runs at different fields intensities were made, and the linear relation between intensity and stream velocity (Figure 5) was used to refer all values to the same acoustic field intensity. By defining the streaming speed at z = A in db as

$$10 \log_{10}\left(\frac{u_{20A}}{u_{20R}}\right)$$

and using the reference velocity $u_{20R} = 1.00$ cm/sec, the axial stream-

ing speeds at different distances, z, from the source can be plotted in db re 1.00 cm/sec. This is shown in Figure 11. The change in speed per unit distance,

$$\Sigma = (1/Z)\ 10\ \log_{10}\left(\frac{u_{20B}}{u_{20A}}\right) \tag{22}$$

is defined as the axial streaming attenuation. The value of Σ is observed from Figure 11 to be 0.165 db/cm.

In order to determine the causes of this stream attenuation, the equation which predicts the axial streaming velocity may be written, for a given axial position A, as

$$u_{20A} = G_A P_{10A}^2\ C \tag{23}$$

or, for position B, as $u_{20B} = G_B P_{10B}^2\ C$

The letter G represents a factor which takes into account the variation of u_{20} with geometrical form of the acoustic field, at constant axial intensity P_{10}^2. C is a constant.

Forming the ratio, taking the log to the base ten, and dividing by the separation $z = z_B - z_A$, there results

$$(1/Z)\ 10\ \log_{10}\frac{u_{20B}}{u_{20A}} = (1/Z)\ 10\ \log_{10}\left(G_B/G_A\right) + (1/Z)\ 20\ \log_{10}\frac{P_{10B}}{P_{10A}}$$

$$\Sigma = \delta + \alpha \tag{24}$$

Equation (24) describes the axial streaming attenuation in db per unit distance as caused by an equivalent attenuation due to a divergence of the acoustic beam, δ, and a real acoustic intensity attenuation, α, due to absorption of acoustic energy. Such a presentation relies on the validity of using a perturbation of the Eckart solution to take account of the changing field at different distances

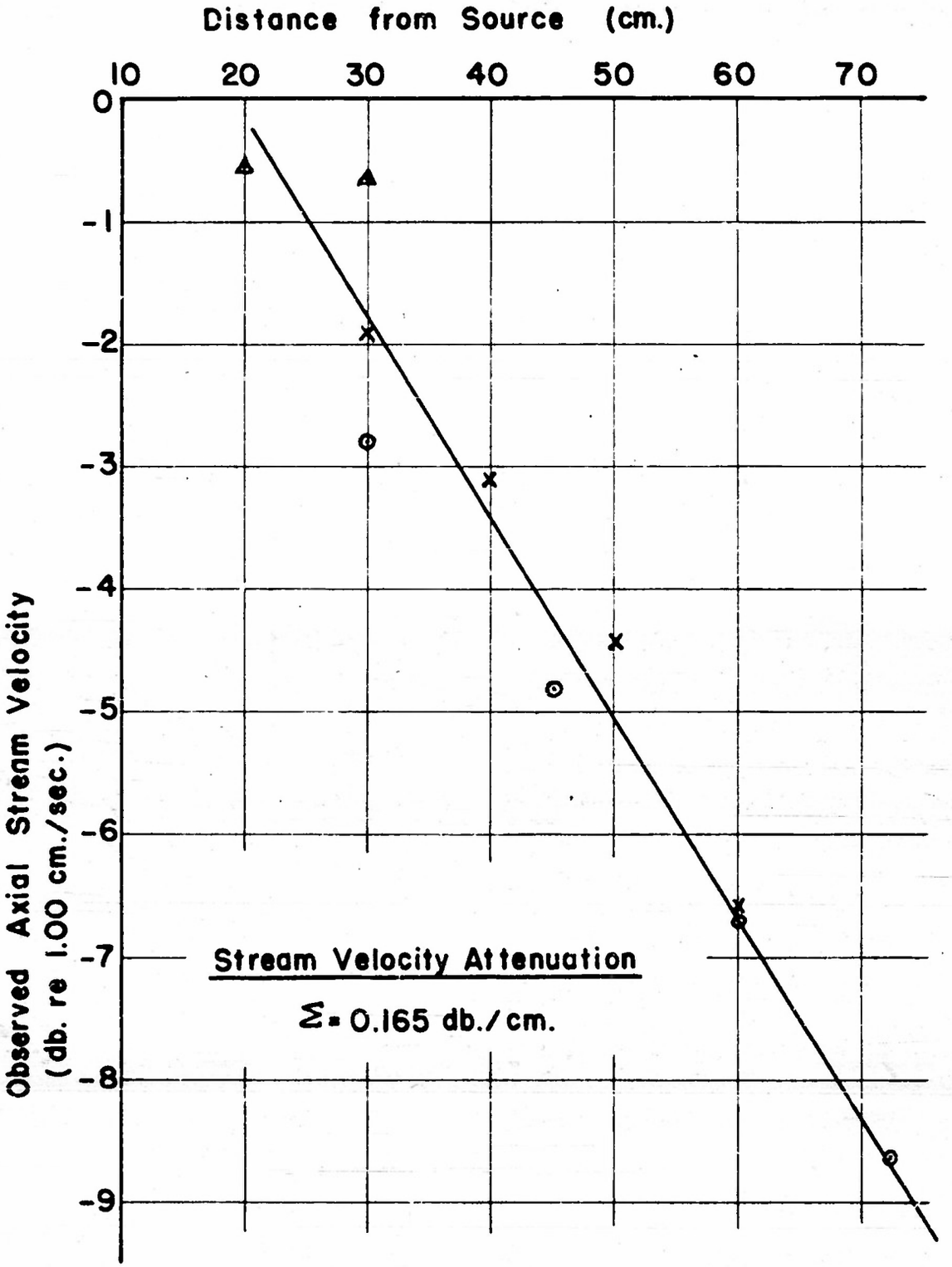
Distance from Source (cm.)
10
20
30
40
50
60
70
0
-1
-2
-3
-4
-5
-6
-7
-8
-9
Observed Axial Stream Velocity
(db. re 1.00 cm./sec.)
Stream Velocity Attenuation
Σ = 0.165 db./cm.

FIG. 11

from the source. This point is discussed in Appendix B.

To calculate the term due to change of the acoustic geometry, the acoustic field was recorded at 26 cm, 50 cm, and 72 cm from the source. At each distance from the source the microphone probe was moved through four different diameters and these responses averaged to give the average distributions shown in Figure 9. All records were taken with the recorder potentiometer adjusted so that the recorder deflected full scale for the pressure on the axis, P_{10}. But these axial pressures would not be equal, even on the assumption of no attenuation. Rather, the energy transmitted through any cross-section of the tube should be the same if there is no attenuation. So $\int_o^{r_o} r P_{10}^2 \, dr$ was computed graphically, from curves such as in Figure 7, for these three different cross-sections to give:

$$\int_o^{r_o} r P_{10}^2 \, dr = 0.0268 \, P_{107}^2 \, r_o^2$$
$$= 0.0149 \, P_{105}^2 \, r_o^2$$
$$= 0.0073 \, P_{102}^2 \, r_o^2$$

To "normalize" with respect to the intensity at 72 cm:

$$P_{102}^2 = 3.67 \, P_{107}^2 \qquad (25)$$
$$P_{105}^2 = 1.80 \, P_{107}^2$$

Next, the axial stream velocity was calculated by graphical integration of $\int_o^{r_o} q \, P^2(r) \, dr$ from curves such as in Figure 8, with the results:

$$u_{202} = 0.0345\ KP_{107}^{2}\ r_o^2 = 2.83 \text{ db re } u_{207}$$

$$u_{205} = 0.0261\ KP_{107}^{2}\ r_o^2 = 1.62 \text{ db re } u_{207} \qquad (26)$$

$$u_{207} = 0.0180\ KP_{107}^{2}\ r_o^2 = 0 \text{ db re } u_{207}$$

These velocities are plotted in Figure 12. The attenuation of the axial stream velocity due to divergence of the acoustic beam is observed to be

$$\delta = 0.062 \text{ db/cm.}$$

The term $\alpha = (1/Z)\ 20 \log_{10} \frac{P_{10B}}{P_{10A}}$ is the sound intensity attenuation per unit distance. The value $\alpha = 0.078$ db/cm for air at 185 KC given by the classical theory is generally conceded to be too low, because only shear viscosity and thermal conductivity are considered as sources of energy loss. Beyond this, there is general and great disagreement about the magnitude of the correction to the classical formula. The work of Sivian[14] is frequently quoted in the literature. He gives $\alpha = 0.118$ db/cm for dry air and $\alpha = 0.144$ db/cm for air with 1.26% H_2O molecules, but states that his data are "subject to an r.m.s. spread of the order of 25%." More recent work[15] leads to a slightly lower value for moist air. The experiments described in this section were performed using air of approximately 1% H_2O molecules. The value of the acoustic intensity attenuation, α, when added to the divergence attenuation factor, δ, should lead to the axial streaming attenuation, Σ.

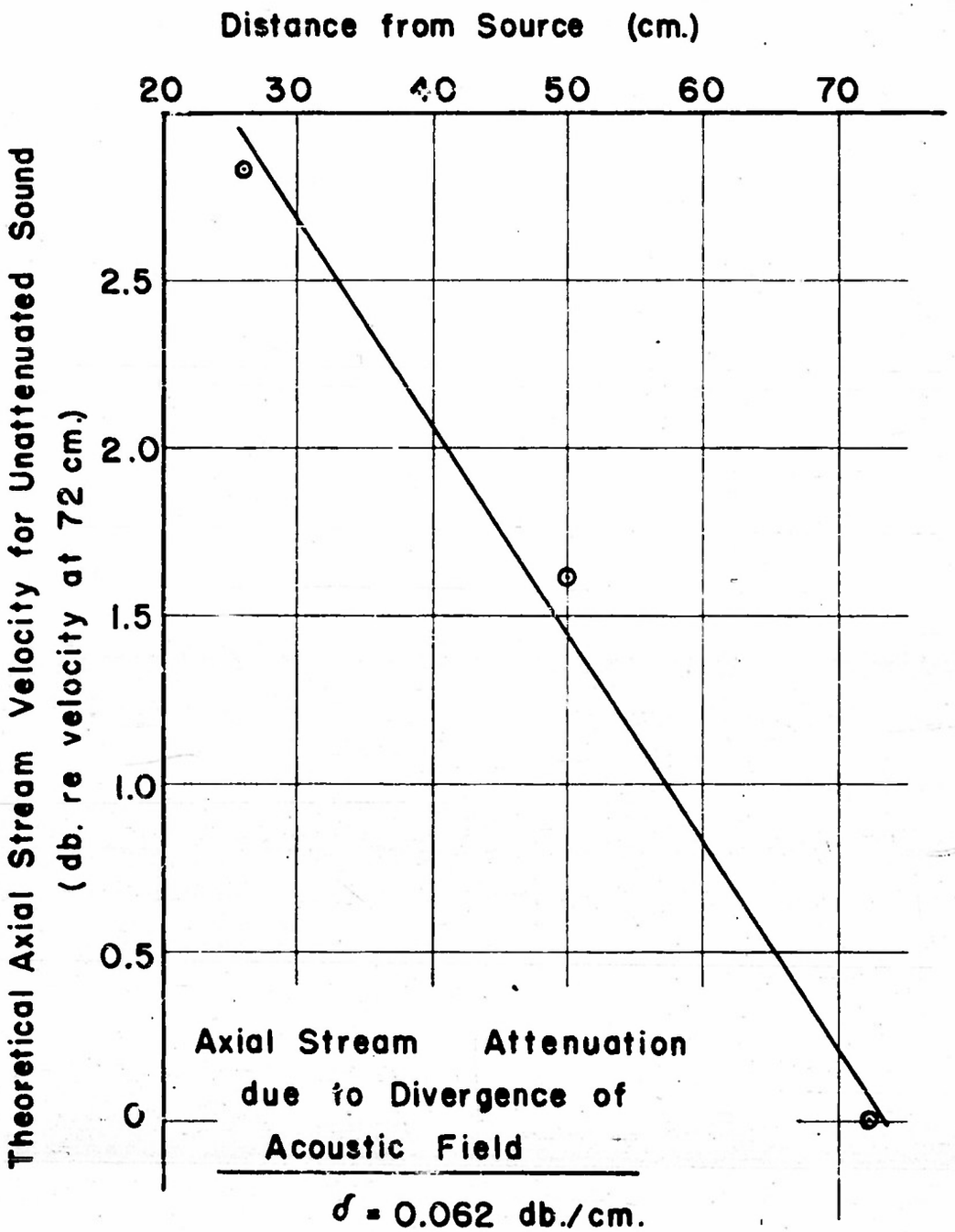
Distance from Source (cm.)
20
30
40
50
60
70
Theoretical Axial Stream Velocity for Unattenuated Sound
(db. re velocity at 72 cm.)
2.5
2.0
1.5
1.0
0.5
0
Axial Stream Attenuation
due to Divergence of
Acoustic Field
α = 0.062 db./cm.

FIG. 12

Source	% H_2O	α db/cm.	δ db/cm.	$\Sigma = \alpha + \delta$ db/cm.	% Discrep.
Sivian Moist Air	1.26	0.144	0.062	0.208	+ 25
Penn State Moist Air	1.00	0.126	0.062	0.188	+ 14
Sivian Dry Air	0	0.118	0.062	0.180	+ 9
Classical Dry Air	0	0.078	0.062	0.140	- 15

The values in the fourth column are compared with the observed axial streaming attenuation, $\Sigma_{OBS.} = 0.165$ db/cm.

Summarizing: the observed axial stream attenuation of 0.165 db/cm in moist air can be accounted for by the change in the acoustic field intensity and geometry as the sound wave proceeds away from the source. The effect is not a local one at the source, but takes place in the medium.

C. DEPENDENCE OF STREAMING ON THE MEDIUM

Having verified that introduction of thermal conductivity into the definition of b^* gives an excellent agreement between b^* obtained by streaming and the value from attenuation measurements for argon, one looks for a similar situation for other gases, too.

Continuing the analysis of b^* as including all attenuative mechanisms, the non-classical part of equation (19) may be written

$$\mu'_{NC} = \frac{2 \rho c \alpha_{NC}}{k^2} \tag{27}$$

where the classical effects of heat conductivity and shear viscosity have been subtracted out.

The mechanism of molecular relaxation has been successful in

explaining the non-classical absorption for many gases, and the amplitude attenuation in nepers per unit length by this process is

$$\alpha_M = 1/2 \frac{C_i}{C_v} \frac{\gamma - 1}{c_o \gamma} \frac{k_{10} \omega^2}{k_{10}^2 + \omega^2} \tag{28}$$

where C_i = internal specific heat

C_v = specific heat at constant volume

c_o = speed of sound

γ = ratio of specific heats

$k_{10} = 2\pi f_{10}$ = angular relaxation frequency

$\omega = 2\pi f$ = angular acoustic frequency at which molecular attenuation is α_M

The process described by equation (28) considers that there is a relaxation frequency for a given intra-molecular process (vibration or rotation) such that when the fluid is excited by a sound wave at this frequency, there is a maximum acoustic attenuation per wavelength. This energy loss is due to the molecules being set into vibration (or rotation) and, because of the time lag necessary for taking up and returning this energy, the energy comes back to the translational mode out of phase with the sound wave, and is thereby degenerated into heat. For lower or higher acoustic frequencies than this relaxation frequency, the loss of energy per cycle is less. Presumably such a process would show up as the λ or μ' of the macroscopic hydrodynamic equations (1) or (2). From the results of section II-B-3 it is clear that the monatomic gas argon has zero bulk viscosity. This section shall study the question of whether there is an inherent bulk viscosity in the gases dry nitrogen and moist air, or whether the bulk

viscosity is composed solely of the contribution due to intramolecular processes.

Equations (27) and (28) lead to

$$\mu'_M = \frac{\gamma}{2\pi^2} p \frac{c_o \alpha_M}{f^2} = p \frac{C_i}{C_v} (\gamma-1) \frac{k_{10}}{k_{10}^2 + \omega^2} \qquad (29)$$

where p = atmospheric pressure

μ'_M = bulk viscosity due to molecular relaxation

The value of μ'_M is seen to reduce to

$$\mu'_M = p \frac{C_i}{C_v} \frac{\gamma-1}{k_{10}} = \text{a constant} \qquad \text{for } \omega << k_{10} \qquad (30)$$

or $$\mu'_M = p \frac{C_i}{C_v} \frac{(\gamma-1)\, k_{10}}{\omega^2} \qquad \text{for } \omega >> k_{10} \qquad (31)$$

So the value of μ'_M is zero for very high frequencies with respect to the relaxation frequency and climbs through the relaxation frequency to reach a steady value for all frequencies much less than the relaxation frequency. Schematically:

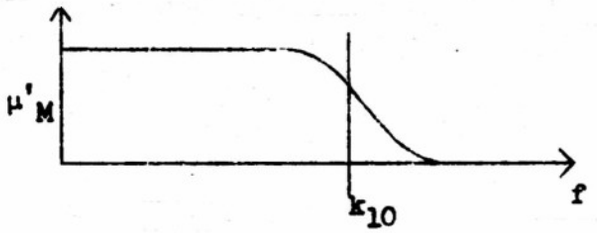

Nitrogen

The streaming experiment was conducted at 185 KC and so one would expect contributions to μ'_M from both vibrational relaxation which occurs[16] strongly in the region 15 KC to 25 KC, and from rotational relaxation which occurs in the 450 megacycle region. Schmidt-müller observed attenuations from 20 KC to 100 KC in nitrogen. He found that the excess (above classical) absorption could be explained

equally well as being due to either:

A) a vibrational relaxation frequency at 25 KC, or

B) a vibrational relaxation frequency at 15 KC, superimposed on an "excess classical" absorption of 15%.

On the basis of his hypothesis A), and using his constants:

$$C_1 = 0.0029 \qquad f_{10} = 25 \text{ KC}$$

$$C_v = 5.0 \qquad f = 185 \text{ KC}$$

$$\gamma = 1.40$$

there results $\mu'_{MV}/\mu = \frac{p}{2\pi} \frac{C_1}{C_v} \frac{(\gamma-1)}{\mu} \frac{f_{10}}{f_{10}^2 + f^2} = 0.151$

where μ'_{MV} is the bulk viscosity contribution due to molecular vibration.

Or using his hypothesis B), in which the vibrational relaxation frequency, f_{10}, is assumed to be 15 KC, there results

$$\mu'_{MV}/\mu = 0.10 \qquad \text{and} \qquad \mu' \text{ Excess classical}/\mu = 0.26$$

Values of $\mu'_{M}/\mu = \frac{\mu'_{MV} + \mu'_{MR}}{\mu}$ from attenuation or streaming experiments are obtained by subtracting $b_{class} = 4/3 + \frac{(\gamma-1)\kappa}{\mu C_p} = 1.85$ from the value of b^* as defined by equation (19). These values are all for the frequency 185 KC. They are tabulated below:

Table I

b^*	μ'_{M}/μ	Source
2.00	0.15	Schmidtmuller, hypothesis A)
2.18	0.33	Streaming
2.21	0.36	Schmidtmuller, hypothesis B)

Clearly, the streaming experiment supports hypothesis B) in preference to hypothesis A). But, at the same time, the 15% correction to classical attenuation now demands "une raison d'etre."

One would expect that when Schmidtmuller adds 15% to his classical attenuation he is taking account of the contribution of rotational relaxation, so that $\mu'_{\text{excess classical}}$ should be labeled μ'_{MR}. Today, following the work of Zmuda[17] and Parker,[13] this correction should be on a better experimental basis. The Parker attenuation experiment used a progressive pulse method with frequencies from 60 KC to 70 KC in the range 5 to 50 megacycles per atmosphere. The work by Zmuda was performed by interferometer at the frequency 3 megacycles per second in the range 3 to 109 megacycles per atmosphere, and shows the beginnings of rotational relaxation towards the higher f/p values. Although the frequency ranges of these two experiments overlap, the results show a real discrepancy, the Parker work giving the ratio of experimental attenuation to classical attenuation as 1.25, while Zmuda gives 1.40. The lower frequencies of both experiments are sufficiently small with respect to the rotational relaxation frequency for μ'_{MR} to be given by the constant of equation (30). The Parker results are probably the more reliable of the two because a) the validity of the measurements was first verified by a successful determination of the attenuation in argon, and b) the value of the ratio, experimental attenuation divided by classical attenuation, is close to 1.2 which is the result to be expected from classical kinetic theory for rotational relaxation.[18] The Parker value of the rotational relaxation frequency will be used to calculate the

value of μ'_{MR}.

$$\mu' MR/\mu = \frac{p}{\mu} \frac{Ci}{Cv} \frac{(\gamma-1)}{k_{10}} = 0.31$$

where $k_{10} = 2.88 \times 10^9 \text{ sec}^{-1}$

$C_i = R$

$C_v = 5/2R$

$\gamma - 1 = 0.40$

$p = 1.013 \times 10^6 \text{ dyne/cm}^2$

This value is equivalent to 17% of $b_{classical} = 1.85$ and, therefore, reinforces the argument for hypothesis B).

One may conclude that the results of Schmidtmüller, Parker and this streaming experiment concur, and that the attenuation of sound in dry nitrogen is due to the classical loss mechanisms of heat conductivity and shear viscosity, plus losses due to a vibrational relaxation frequency at approximately 15 KC and a rotational relaxation frequency at approximately 450 megacycles. This streaming experiment provides no evidence of an inherent bulk viscosity which is distinct from relaxation contributions.

Moist Air

In the case of moist air of 1.35% H_2O molecules, there is available the data of attenuation experiments at Pennsylvania State College[15] and the correction for molecular absorption due to H_2O given by Kneser.[19] The value of b^* obtained from streaming falls between these two values, again supporting the argument that the streaming experiment is another method for obtaining attenuation constants. The three values of b^* are given below, in Table II.

Table II

b^*	Source
2.45	sum of classical plus Kneser molecular attenuation
2.59	streaming
2.83	Penn State

III. CONCLUSIONS

The work of Eckart, which considers the vorticity generated in a viscous medium during passage of a sound beam, has been extended to consider "surface sources" of vorticity which appear when the sound beam makes contact with a solid, restraining surface. As in the Eckart work, the dynamic shear viscosity coefficient, μ, is assumed to be independent of the density changes which accompany a sound wave. However, the effect of a density dependent bulk viscosity coefficient is investigated, and it is found that the sources of vorticity are unaffected.

A guided, progressive wave in which $\lambda_{viscous} << \text{tube radius} \tilde{<} \lambda_{acoustic}$ has been studied. The predominant sources of vorticity in this case are the "surface sources," and the resultant acoustic streaming is controlled by these "surface sources."

A radially-symmetric progressive acoustic beam has been set up in a closed, gas-filled tube to cause streams driven by the Eckart, volume, source of vorticity. A careful determination of the acoustic pressure at all points of a cross-section of the beam has been used to successfully predict the stream velocities at this cross-section, for argon. The work with argon and the results of further experiments with dry nitrogen and moist air indicate that:

1) the Navier-Stokes equation, the equation of continuity, and the "acoustic equation of state," $p_1 = \rho_1 c_o^2 + A\rho_1^2$, provide a valid basis for second-order studies of streaming;

2) thermal conduction effects may be introduced into the Eckart streaming equations in the same manner as they appear in the attenuation formulas;

3) the macroscopic quantity, bulk viscosity, is made up of contributions from the intra-molecular processes of vibrational and rotational relaxation.

IV. ACKNOWLEDGEMENT

The author is indebted to Dr. I. Rudnick for his guidance and encouragement during the course of this study. He also wishes to acknowledge helpful discussions with Dr. Carl Eckart and Dr. Robert Leonard.

BIBLIOGRAPHY

BIBLIOGRAPHY

1. C. Eckart, Phys. Rev. 73, 68 (1948).
2. Lord Rayleigh, Theory of Sound (Dover Publications, New York, 1945), Vol. II, p. 353.
3. K. Schuster and W. Matz, Akust. Zeits. 5, 349 (1940).
4. H. Schlichting, Phys. Zeits. 33, 327 (1932).
5. H. Lamb, Hydrodynamics (Dover Publications, New York, 1945), Article 328.
6. K. U. Ingard and S. Labate, J. Acoust. Soc. Am., 22, 211 (1950).
7. S. Goldstein, Modern Developments in Fluid Dynamics (Oxford Press, England, 1938), Vol. I, p. 319.
8. L. Liebermann, Phys. Rev. 75, 1415 (1949).
9. J. J. Markham, Phys. Rev. 86, 497 (1952).
10. F. E. Fox and L. F. Herzfeld, Phys. Rev. 78, 156 (1950).
11. W. Nyborg, J. Acoust. Soc. Am. 25, 68 (1953).
12. J. C. Maxwell, Phil. Trans. clvii, 49 (1866).
13. J. G. Parker, C. Adams, R. Stavseth, J. Acoust. Soc. Am., 25, 263 (1953).
14. L. J. Sivian, J. Acoust. Soc. Am., 19, 914 (1947).
15. Pennsylvania State College, Report on Atmospheric Physics and Sound Propagation (1950), p. 160.
16. N. Schmidtmüller, Akust. Zeits, 3, 115 (1938).
17. A. J. Zmuda, J. Acoust. Soc. Am., 23, 472 (1951).
18. W. L. Nyborg and J. F. S. Y. Lee, J. Acoust. Soc. Am., 25, 821 (1953)
19. H. O. Kneser, Akust. Zeits. 5, 256 (1940).
20. Lord Rayleigh, Theory of Sound (Dover Publications, New York, 1945), Vol. II, p. 324.

APPENDIXES

Appendix A

STREAMING CAUSED BY A PLANE PROGRESSIVE WAVE IN A CYLINDRICAL TUBE

The purpose of this appendix is to compare the relative magnitudes of the surface and volume sources of streaming for a guided plane progressive wave in a cylindrical tube.

In order to assess the relative importance of the sources of vorticity represented by the three terms on the right of equation (5), it is convenient to present the equation, in so far as possible, in terms of the first order acoustic particle velocity, $\vec{u}_1$, or its curl, $\vec{R}_1$. Using (2) and (3), gives.

$$\nabla^2\vec{R}_2 = -(b/c_o^2)(\partial\vec{u}_1/\partial t \times \nabla\nabla\cdot\vec{u}_1) - [b\nu_o/c_o^2]\,[(\nabla\times\vec{R}_1)\times\nabla\nabla\cdot\vec{u}_1] \qquad (32)$$
$$-(1/\nu_o)\nabla\times(\vec{u}_1\times\vec{R}_1) + (1/\nu_o)(d\nu/d\rho)_o\nabla\times[\rho_1(\nabla\times\vec{R}_1)]$$

In equation (32) the first two sources of vorticity have come from the term $\vec{S}_R$. Identifying the second as "$\vec{A}$" and comparing with the third term, $\vec{S}_R$, in equation (32), "$\vec{A}$" can be shown to be generally negligible.

Expanding: $\vec{A} = [-b\nu_o/c_o^2]\,[(\nabla\times\vec{R}_1)\times\nabla^2\vec{u}_1]$

while $\vec{S}_R = (1/\nu_o)\,[(\nabla\times\vec{R}_1)\times\vec{u}_1]$

Therefore: $|\vec{S}_R|/|\vec{A}| = (1/\nu_o)/(\nu_o b k_o^2/c_o^2) = (4/b)(\lambda_{acous.}/\lambda_{visc})^4$

where $\lambda_{acous} = 2\pi/k_o$ $\qquad$ $\lambda_{visc} = 2\pi\,(2\nu_o/\omega)^{1/2}$

Since it is generally true that the viscous wave length is much less than the acoustic wave length in fluids,* the "$\vec{A}$" term will henceforth be dropped and what is left of $\vec{S}_E$ will be called $\vec{S}_e$. Then the vorticity equation may be written:

$$\nabla^2\vec{R}_2 = \underbrace{+(-b/c_o^2)(\partial\vec{u}_1/\partial t \times \nabla\cdot\vec{u}_1)}_{\vec{S}_e} + \underbrace{(-1/\nu_o)[\nabla\times(\vec{u}_1\times\vec{R}_1)]}_{\vec{S}_R} + \underbrace{(1/\nu_o)(d\nu/dp)_o\nabla\times[p_1(\nabla\times\vec{R}_1)]}_{\vec{S}_T} \qquad (33)$$

To proceed further, it is necessary to specify the boundary conditions of the particular problem, so that expressions for $\vec{u}_1$ and p_1 may be presented. A search of the literature reveals no exact solution to the Navier-Stokes equation in cylindrical coordinates, although preliminary equations have been set up by Kirchoff and reproduced by Rayleigh[20] for the case of a guided plane progressive wave in a cylindrical tube. One of the constants of integration is evaluated by the condition that the particle velocity be zero on the tube walls. The solution based on $\beta >> \frac{1}{R} \approx k$ then becomes:

$$\text{Axial Velocity, } W_1 = A\{J_o[(-1+i)\beta r] - J_o[(-1+i)\beta R]\} \qquad (34)$$

$$\text{Radial Velocity, } U_1 = [Ak(1-i)/(2\beta)]\{-J_1[(-1+i)\beta r] + (r/R)J_1[(-1+i)\beta R]\} \qquad (35)$$

where:

ω = angular frequency of the acoustic wave

$k = 2\pi/\lambda_{acous.}$ = acoustic wave number

R = tube radius

---

*For example, for a monatomic gas $\lambda_{visc} << \lambda_{acous}$ as long as the period of the sound wave is long compared to the time between atomic collisions.

r = distance from tube axis

h = R-r = distance from tube wall

$\beta = \sqrt{\omega/2\nu}$

$\nu = \mu/\rho$ = kinematic shear viscosity.

An approximate form of this solution, which holds for r = 0 and for $\beta r > 1$, for a wave propagated in the +z, $\vec{i}_3$, direction and of velocity $\vec{u}_1 = u_{10}\cos(kZ-\omega t)\vec{i}_3$ on the axis is:

$$W_1 = u_{10}\{\cos(kZ-\omega t) - e^{-\beta h}\cos(kZ-\omega t-\beta h)\}$$

$$U_1 = [(u_{10}k)/\sqrt{2}\beta]\{(r/R)\cos(kZ-\omega t+\pi/4) - e^{-\beta h}\cos(kZ-\omega t-\beta h+\pi/4)\} \qquad (36)$$

The assumed solution is seen to have a radial as well as an axial component, both with a precipitous drop in the particle velocity through the thin boundary layer near the wall. β is a large number (e. g. for f = 1000 cps in air, $\mu = 2 \times 10^{-4}$ poises, $\beta \sim 200.\ cm^{-1}$). Further, the radial component is smaller than the axial by virtue of the factor k/β which, for the example given, would be about 10^{-3}.

Expanding all vorticity sources in cylindrical coordinates r, θ, Z when there is axial symmetry all derivatives with respect to θ may be set equal to zero. Then, denoting the unit vector in the θ direction by $\vec{i}_2$:

$$\vec{s}_e = -(b/c_o^2)(\partial\vec{u}_1/\partial t \times \nabla\nabla\cdot\vec{u}_1) = \vec{i}_2(-b/c_o^2)\{-U_t[U_{rz} + (1/r)U_z + W_{zz}] + W_t[U_{rr}+(1/r)U_r - U/r^2 + W_{zr}]\} \qquad (37)$$

$$\vec{s}_R = -(1/\nu_o)\nabla\times(\vec{u}_1\times\vec{R}_1) = \vec{i}_2(-1/\nu_o)\{-W\,U_{zz} - W_z U_z + WW_{rz} + W_z W_r - UU_{rz} - U_r U_z + UW_{rr} + U_r W_r\}$$

$$\vec{S}_T = -1/\rho_o \nabla x(\rho_1 \nabla x \vec{R}_1) = -(\vec{i}_2/\rho_o)\{-\partial\rho_1/\partial r\,[U_{rz}-W_{rr}+U_z/r-W_r/r] - \partial\rho_1/\partial z\,[U_{zz}-W_{zr}] + \rho_1\,[-U_{zzz}+W_{zzr}-U_{rrz}+W_{rrr}-U_{rz}/r+U_z/r^2+W_{rr}/r-W_r/r^2]\}$$

where the short-hand notation $U_{rz} \equiv \partial^2 U/\partial r\partial z$, $W_{rr} \equiv \partial^2 W/\partial r^2$ etc.

Using equations (36) for the evaluation, a large number of quadratic terms are formed. Of these, only the ones with a non-zero time average value are of interest in a discussion of streaming; the second harmonic terms are dropped.

For the conditions $\beta > 1/r > k$ there results:

$$\vec{S}_e = -\vec{i}_2(b\beta' k^2 u_{10}^2/c_o)\{-e^{-2\beta h} + e^{-\beta h}[\sin\beta h + \cos\beta h] + k^2 r/4\beta^2 R)\}$$

$$\vec{S}_R = -\vec{i}_2(\beta k u_{10}^2/\nu_o)\{e^{-2\beta h} - e^{-\beta h}[(r/R)(\sin\beta h+\cos\beta h)]\} \qquad (38)$$

$$\vec{S}_T = -\vec{i}_2(\beta k u_{10}/\nu_o)\left\{\frac{1}{\sqrt{2}\,\beta r}\, e^{-2\beta h} - \frac{1}{2}\, e^{-\beta h}(\sin\beta h-\cos\beta h)\right\}$$

It is noted that the terminology adapted for the sources of vorticity is supported by the presence of b (which involves bulk viscosity) only in the volume term, $\vec{S}_e$. The sources of vorticity are similar in their variation within the boundary layer but only the volume source $\vec{S}_e$ has a term which takes on significant values even away from the wall. It is of interest to compare the orders of magnitude of the sources of vorticity and it appears that:

$$\frac{|\text{Surface Sources}|}{|\text{Volume Source}|} \simeq \frac{c_o^2}{b\omega\nu_o} \simeq 1/(\omega\tau)$$

Where $\tau = (4/3)\nu_o/c_o^2$ = "viscous relaxation time" as used by Eckart, and

is of the same order of magnitude as the time between collisions for a monatomic gas.

Since the magnitude of the volume source of vorticity is proportional to frequency and the surface terms are not, one looks for a frequency at which the volume source would become of importance for a sound beam which fills the tube. Apparently this would occur when the frequency approaches $(1/\tau)$. However, it should be pointed out that the equations (36) on which this conclusion is based are valid only if $\lambda_{visc} << R \tilde{<} \lambda_{acoust}$. But within these limits, the surface sources of vorticity appear more important than the volume source.

But the answer to the obvious question of whether the streaming, say on the axis, is controlled by the surface sources and in the same ratio as above, requires an integration of equations (38). A vector potential defined by $\nabla^2 \vec{A}_2 = -\vec{R}_2$ (where $\vec{A}_2$ is a solenoidal vector) is proposed. Then $\vec{u}_2 = \nabla \times \vec{A}_2$ for an incompressible fluid. (Note: It is assumed that $|\vec{u}_2| << C_o$ so that the streaming flow is incompressible.) For the geometry considered here, $\vec{u}_2 = f(r)\,\vec{i}_z$ and $\vec{A}_2 = g(r)\vec{i}_2$ where $\vec{i}_2$ and $\vec{i}_z$ are the unit vectors in the θ and z (axial) directions, respectively. The proposal $A_\theta = r^q$ yields the solution to the homogeneous equation, $\vec{A}_2 = (ar + br^3)\vec{i}_2$. It is observed that the major sources of vorticity are near the wall and so the assumption is made that only the variation of $\vec{A}_2$ in the r direction near the wall is significant in determining the particular integral. Therefore, for the determination of the particular integral $+\nabla^2(-\nabla^2 \vec{A}_2)$ is replaced by $d^4A_\theta/dh^4 = d^4A_\theta/dr^4$. After integration, the two constants are evaluated by the two conditions:

(a) $W_2 = 0$ at the tube wall

(b) $\int_0^R W(r)\, r\, dr = 0$ for mass continuity through a cross section of the tube.

The Poisson's equation is solved first with $\vec{S}_e$ as the driving term to yield:

$$W_{2e} = + [bk^2u_{10}^2/4\beta^2c_o)] \{[k^2\beta R^3/5][r^4/4R^4 - r^2/3R^2 + 1/12] - 1/2[1-2r^2/R^2]\} \quad (39)$$

Then the Poisson's equation is solved with $\vec{S}_R$ as the source of vorticity to give:

$$W_{2R} = - (u_{10}^2/4c_o)\ (1-2r^2/R^2) \quad (40)$$

Finally, both surface sources of vorticity $\vec{S}_R + \vec{S}_T$ are set up as the driving terms, with the result:

$$W_{2R+2T} = - (3u_{10}^2/4c_o)\ (1-2r^2/R^2) \quad (41)$$

Only the streaming outside of the boundary layer is reported above.

Study of these three results reveals that the ratio of the magnitudes of the two types of streams at the tube axis is approximately:

$\frac{W_{2R+2T}}{W_{2e}} \approx \frac{c_o^2}{b\nu_o\omega^2}$ and so the streaming velocity in this case is clearly dominated by the surface sources.* However, this conclusion must not be extended to the case of a sound beam ($R \gg \lambda_{ac}$.) which

---

*Since $kR \lesssim 1$ and $R\beta >> 1$, it is possible that the first term in the W_{2e} brackets may be greater or less than the second term, and could even result in W_{2e} being zero on the axis.

does not fill the tube. Then, as Eckart points out, the volume source would generate extremely great stream velocities as the ratio (beam radius/tube Radius)$\to$0. It might be expected that an experimental sound beam, such as described earlier in this paper, might be strong enough at the tube walls to cause a surface source of vorticity which would dominate the flow but this is not the case. Forming the ratio of:

$$|u_{20}|_{\text{Eckart}} = \frac{.02bk^2}{2\,P_o^2 c_o^3} P_{1\,\text{axis}}^2 r_o^2 \tag{13}$$

$$\text{to } |u_{20}|_{\text{Surface}} = \frac{u_{10}^2}{4c_o} = \frac{P_{1\,\text{wall}}^2}{4\rho_o^2 c_o^3} \tag{35}$$

there results:

$$\frac{|u_{20}|_{\text{Eck}}}{|u_{20}|_{\text{Surf.}}} = \frac{4bk^2 r_o^2 P_{1\,\text{axis}}^2}{P_{1\,\text{wall}}^2}$$

It is clear that for a real sound beam in which $kr_o >> 1$ and $P_{1\,\text{axis}} > P_{1\,\text{wall}}$, the Eckart source of vorticity controls the axial streaming.

Equations 39-41 present another fact; that $\vec{S}_e$, in general, causes axial flow away from the sound source while $\vec{S}_R$ and $\vec{S}_T$ cause streaming away from the sound source at the walls, returning <u>towards</u> the source at the axis. The apparent contradiction is reconciled when one considers that $\vec{S}_e$ is concerned with energy loss and transfer of acoustic momentum into streaming momentum within the medium. The surface terms, on the other hand, take account of the transfer of momentum as the sound energy is dissipated within the boundary layer at the tube walls.

A final observation is that the streaming velocity prediction is increased when both $\vec{S}_R$ and $\vec{S}_T$ are used as driving sources. The cause

of this increase is recognized if the time average of $\vec{S}_T$ is written as:

$$\langle \vec{S}_T \rangle = \left\langle \frac{\rho_1}{\rho_o} \nabla x(\nabla x \vec{R}_1) \right\rangle - \left\langle \frac{1}{\rho_o} \nabla \rho_1 x(\nabla x \vec{R}_1) \right\rangle$$

$$= -\left\langle \frac{1}{\nu_o} (\nabla \cdot \vec{u}_1)(\nabla x \vec{u}_1) \right\rangle - \left\langle \frac{1}{\omega^2} \nabla\nabla \cdot \vec{u}_1 x (\nabla x \vec{R}_1) \right\rangle$$

Then $\vec{S}_T$ shows up as dependent on the compressibility of the medium, as well as the irrotationality. This contrasts with $\vec{S}_R$ which is a function of the irrotationality of the medium, only.

APPENDIX B

VALIDITY OF THE ATTENUATION APPROXIMATION

The Eckart solution, which is the basis of this experimental work, requires the inclusion of viscosity in the force equations. Later, for the special case of the "ideal" beam, the effects of both viscosity and diffraction on the first-order acoustic pressure are considered to be negligible, and the equation of the unattenuated, non-divergent sound beam is written as $p_1 = P(r) \sin (kz - \omega t)$. Further, Eckart has assumed that there are no end effects. The resulting solution describes the streaming as independent of longitudinal position, z.

Experimentally, since the streaming at the center of the face of the sinusoidally vibrating disk must be zero, there is a region near the source where the axial stream velocity rises rapidly from zero to a maximum value. Similarly, the axial stream velocity must drop to a zero value at the fixed end plate. Within these two regions, the streams have strong radial components and the Eckart solution cannot be expected to be valid. Telescopic observation showed that the streaming was predominantly longitudinal in the region from 20 cm to 75 cm from the source in this experiment, and all data were taken within this region. The distance from source to absorbing end plug was about 100 cm.

Even this central region does not fulfill the conditions of the

Eckart solution because of attenuation, divergence and non-planar character of the sound wave. The latter two conditions would be difficult to take account of, and are probably not as influential as the attenuation in the present experiment (see table on top of page 42 where the non-planar effect is included in the geometrical divergence term δ). The attenuation could be described by using $p_1 = P_1(r) \sin(kz - \omega t)\, e^{-\alpha z}$ where α is the amplitude attenuation coefficient. Substitution into $\vec{S}_E$ of the vorticity equation (5) leads to

$$\nabla^2 \vec{R}_2 = \frac{b\omega k}{2\rho_o^2 c_o^4} \frac{d[P_1^2(r)]}{dr} e^{-2\alpha z} \qquad (42)$$

a vector Poisson's Equation whose solution would show that the streaming velocity for an attenuated beam will have both longitudinal and radial components. The magnitude of the radial component depends on the attenuation α, - becoming zero for the unattenuated sound beam.

The determination of the streaming velocity requires, first, the solution for $\vec{R}_2$. Solutions to the homogeneous equation are sought under the conditions of axial symmetry, regularity at the axis and dependence on both r and z. Such a solution is

$$R_{2\theta} = (-Ae^{\ell z} + Be^{-\ell z}) J_1(\ell r) + Cr + \nabla\phi \qquad (43)$$

where ℓ is a propagation constant for vorticity and $\nabla\phi$ is a potential function which may be introduced to satisfy boundary conditions. The particular integral would not be as easy to find. The complete solution for $\vec{u}_2$ would require the integration of still another, more complex, vector Poisson's Equation, $\nabla^2 \vec{A}_2 = -\vec{R}_2$, where $\vec{A}_2$ is the

solenoidal vector potential whose curl is the streaming velocity, $\vec{u}_2$. The solution will not be attempted here but it should be mentioned that the determination of the constants of integration and the propagation constant for vorticity, ℓ, would have to be evaluated from a knowledge of boundary conditions on velocity.

Without solving this problem, some observations may, nevertheless, be made. It is noted that it is the introduction of attenuation that opens the way to solutions of the type shown in equation (43) where the propagation constant, ℓ, appears for the first time. The greater the attenuation, the more importance must be attached to this propagation constant. For a highly attenuated sound beam, the vorticity, $\vec{R}_2$, generated in one region of the beam can be expected to propagate its influence to adjacent sections. Such a propagation of vorticity does not appear in the Eckart solution precisely because the acoustic field (and the resulting vorticity field) which he treats has no dependence on z and the question of the influence of one cross-section of the flow on the adjacent cross-sections never arises.

In lieu of an analytic solution to this problem, the author has assumed that, within the limits of accuracy of this experiment, the streaming in each section of the tube can be calculated by a knowledge of the acoustic field at this same cross-section. Physically, this assumes that any drag or drive which may be caused by adjacent regions is negligible. Otherwise stated, the attenuation is considered to be large enough to affect the acoustic field but not large enough to cause measurable "coupling" between sections of the streaming field. As one proceeds away from the source (in the middle region where end

effects are negligible) the decrease in axial streaming velocities is accounted for by a relatively small "seepage" of flow into radial components. The substantiation of this explanation is entirely experimental. It is based on these facts:

a) the axial and off-axis streaming predictions at 26 cm from the source for argon and nitrogen coincide (within ± 4%) with predictions based on the observed acoustic field at 26 cm from the source.

b) The axial velocities in the region 20 cm to 75 cm from the source are predicted from a knowledge of (and interpolation and extrapolation from) the observed acoustic fields at 26 cm, 50 cm and 72 cm from the source, with a maximum error of 14% (based on Pennsylvania State College values, loc. cit.).

Within the limits of accuracy of this experiment, as stated above, it is felt that conclusion 4) of page 36 is valid.

DISTRIBUTION LIST

A. Government Distribution
Department of the Navy

Chief of Naval Research
Office of Naval Research
Washington 25, D.C.
Attn: Physics Branch (2 copies)

Director, Naval Research Laboratory
Washington 20, D.C.
Attn: Technical Information Officer (9 copies)

ONR, Branch Offices

Commanding Officer
U.S. Navy Office of Naval Research
Branch Office
50 Church Street
New York 7, New York (1 copy)

Commanding Officer
U.S. Navy Office of Naval Research
Branch Office
American Fore Building
844 N. Rush Street
Chicago 11, Illinois (1 copy)

Commanding Officer
U.S. Navy Office of Naval Research
Branch Office
801 Donahue Street
San Francisco 24, California (1 copy)

Commanding Officer
U.S. Navy Office of Naval Research
Branch Office
1030 E. Green Street
Pasadena 1, California (1 copy)

Office of the Assistant Naval Attache for Research
Navy No. 100
Fleet Post Office
New York, New York (2 copies)

Director
U.S. Navy Underwater Sound Reference Laboratory
Office of Naval Research
P.O. Box 3629
Orlando, Florida (1 copy)

Director
Naval Research Laboratory
Anacostia Station
Washington 20, D.C.
Attn: Sound Division (1 copy)

Director
U.S. Navy Electronics Laboratory
San Diego 52, California

U.S. Naval Academy
Naval Postgraduate School
Physics Department
Del Monte, California
Attn: L. E. Kinsler (1 copy)

Director
Marine Physical Laboratory
University of California
San Diego 52, California

Director
U.S. Navy Underwater Sound Laboratory
Fort Trumbull
New London, Connecticut (1 copy)

Director
David Taylor Model Basin
Carderock, Maryland
Attn: Sound Section (1 copy)

Director
Ordnance Research Laboratory
Pennsylvania State College
State College, Pennsylvania (1 copy)

Chief of the Bureau of Ships
Navy Department
Washington 25, D.C.
Attn: Code 330 (1 copy)
Code 665 (1 copy)
Code 845 (2 copies)

Naval Medical Research Institute
Naval Medical Center
Bethesda 14, Maryland
Attn: Cdr. D. Goldman NMC (1 copy)

Director, Naval Ordnance Laboratory
White Oaks, Maryland
Attn: Sound Division (1 copy)

Woods Oceanographic Institution
Woods Hole, Massachusetts
Attn: Contract Nobsr 43270 (1 copy)

Department of the Air Forces

Commanding Officer
Air Force Cambridge Research Laboratories
230 Albany Street
Cambridge 39, Massachusetts
Attn: Geophysical Research Directorate, ERHS-1

Director
National Bureau of Standards
Division of Mechanics
Washington 25, D.C.
Attn: Dr. R. K. Cook (1 copy)

National Academy of Science
Committee on Undersea Warefare
2101 Constitution Avenue
Washington 25, D.C.
Attn: Dr. John S. Coleman (1 copy)

B. Non-Government Distribution

Massachusetts Institute of Technology
Acoustics Laboratory
Cambridge 39, Massachusetts
Attn: Prof. R. H. Bolt (1 copy)

Harvard University
Cruft Laboratory
Department of Engineering Science and Applied Physics
Cambridge, Massachusetts
Attn: Prof. F. V. Hunt (1 copy)

Catholic University of America
Washington 17, D.C.
Attn: Prof. K. F. Herzfeld (1 copy)

Brown University
Department of Applied Physics
Providence 12, Rhode Island
Attn: Prof. R. B. Lindsay (1 copy)

University of Southern California
Los Angeles 7, California
Attn: Prof. R. E. Vollrath (1 copy)

Norman Bridge Laboratory
California Institute of Technology
Pasadena, California
Attn: Prof. W. G. Cady (1 copy)

University of California
Department of Physics
Los Angeles, California
Attn: Dr. R. W. Leonard (1 copy)

Princeton University
Department of Electrical Engineering
Princeton, New Jersey
Attn: Dr. W. C. Johnson (1 copy)

Case Institute of Technology
Department of Physics
University Circle
Cleveland 6, Ohio
Attn: Dr. R. S. Shankland (1 copy)

Utah University
Salt Lake City, Utah
Attn: Dr. Elsey (1 copy)

Western Reserve University
Department of Chemistry
Cleveland, Ohio
Attn: Dr. F. Hovorka (1 copy)